https://doi.org/10.5194/hess-2024-230
Preprint. Discussion started: 5 August 2024

Hydrology and Earth System Sciences
Open Access
Discussions

Achieving water budget closure through physical hydrological processes modelling: insights from a large-sample study

Xudong Zheng[1], Dengfeng Liu[1*], Shengzhi Huang[1*], Hao Wang[2], Xianmeng Meng[3]

[1]State Key Laboratory of Eco-hydraulics in Northwest Arid Region of China, School of Water Resources and Hydropower, Xi'an University of Technology, Xi'an, 710048, China
[2]State Key Laboratory of Simulation and Regulation of Water Cycle in River Basin, China Institute of Water Resources and Research, Beijing, 100038, China
[3]School of Environmental Studies, China University of Geosciences, Wuhan, 430074, China

Correspondence to: Dengfeng Liu (liudf@xaut.edu.cn)

Abstract. Modern hydrology is embracing a data-intensive new era, information from diverse sources is currently providing support for hydrological inferences at broader scales. This results in a plethora of data reliability-related challenges that remain unsolved. The water budget non-closure is a widely reported phenomenon in hydrological and atmospheric systems. Many existing methods aim to enforce water budget closure constraints through data fusion and bias correction approaches, often neglecting the physical interconnections between water budget components. To solve this problem, this study proposes a Multisource Datasets Correction Framework grounded in Physical Hydrological Processes Modelling to enhance water budget closure, called PHPM-MDCF. The concept of decomposing the total water budget residuals into inconsistency and omission residuals is embedded in this framework to account for different residual sources. We examined the efficiency of PHPM-MDCF and the residuals distribution across 475 CONUS basins selected by hydrological simulation reliability. The results indicate that the inconsistency residuals dominate the total water budget residuals, exhibiting highly consistent spatiotemporal patterns. This portion of residuals can be significantly reduced through PHPM-MDCF correction and achieved satisfactory efficiency. The total water budget residuals have decreased by 49% on average across all basins, with reductions exceeding 80% in certain basins. The credibility of the correction framework was further verified through several noise experiments. In the end, we explored the potential factors influencing the distribution of residuals and found notable scale effects where residuals decrease with increasing basin area. This emphasizes the importance of carefully evaluating the water balance assumption when employing multisource datasets for hydrological inference in small basins.

1 Introduction

Advances in measurement and monitoring techniques have revolutionized the hydrology research through providing an unprecedented opportunity to detect hydrology process (Sivapalan and Blöschl, 2017). Data availability is no longer the key constraint for conducting large-scale research as it once was. Approaches that works with large samples and multisource data are now more attractive for hydrological studies (Nearing et al., 2021). In the absence of satisfactory in-situ observation, we can freely access data from different sources as complement, such as satellite remote sensing, radar, model simulation and reanalysis (Refsgaard et al., 2022). As such, whether at the watershed scale or the modelling scale (e.g., grid cells), we have multiple choices to represent water budget components, thereby facilitating hydrological inferences. This reality is also referred to as the fourth paradigm of hydrology (Peters-Lidard et al., 2017).

However, every coin has two sides, the abundance of available data has brought challenges in data selection, confronting contemporary hydrologists with the task of filtering datasets. After excluding datasets that do not match the research scale and spatiotemporal coverage, we still have no idea about how to select the most suitable one from remaining datasets. In the past decades, extensive efforts have been made to evaluate the accuracy of datasets by referencing in-situ observation or ensemble of multisource data (Sahoo et al., 2011; Tang et al., 2020; Ansari et al., 2022). However, the fact remains that the “true value” is perpetually unattainable, rendering any form of reference data uncertain. For example, the undercatch phenomenon in rainfall measurements is well known, and it is difficult to eliminate the bias even with the application of undercatch corrections (Robinson and Clark, 2020). In terms of the most credible runoff measurements in hydrology, as indicated by recent global research, widespread biases have been revealed (Huang et al., 2023). Therefore, we argue that the evaluation based on reference data lakes sufficient reliability, highlighting the need for more widely applicable criteria in evaluating and correcting datasets from various sources.

The law of mass conservation, typically represented in hydrology by the water balance, constitutes a fundamental principle applicable universally across time and space. Thus, the terrestrial water budget describes the physical consistency among different components of the water balance, which can serve as a criterion for evaluating and correcting datasets. For a closed basin, the water budget can be mathematically expressed as,

$$\frac{\mathrm{d}TWS}{\mathrm{d}t} = P - ET - R, \tag{1}$$

where $\frac{\mathrm{d}TWS}{\mathrm{d}t}$ is change in terrestrial water storage, P is precipitation, ET is evaporation, R is streamflow at the outlet. By incorporating data from different sources into Eq. (1), we can assess whether these data achieve closure of the water budget, thereby evaluating their reliability in depicting hydrological processes. If Eq. (1) is not satisfied, the residual term, known as water budget residuals, can quantify the extent of physical inconsistency among multiple datasets. A comprehensive review of the terrestrial water budget closure examination is given in Lv et al. (2017), interested readers are encouraged to refer to this work. The consensus in the recent scientific literature is that data inconsistency is widespread, attributed to different production processes among various datasets, and no single combination of datasets can fully close the water budget across all basins. Such inconsistency poses an obstacle to robust hydrological inferences. As an example of this, physically inconsistent forcing and evaluation data can mislead hydrological modelling and introduce significant uncertainty to model inferences (Kauffeldt et al., 2013). To mitigate the impact of data inconsistency, it is essential to properly correct datasets and improve water budget closure.

The pioneering work in enhancing water budget closure across different data sources through data correction was conducted by Pan and Wood (2006), who integrated a Constrained Ensemble Kalman Filter (CEnKF) to impose constrains on terrestrial water budget. This technique was subsequently developed and applied in several studies (Sahoo et al., 2011; Zhang et al., 2016). Similar extension methods include Multiple Collocation (MCL) and Proportional Redistribution (PR) method (Abolafia-Rosenzweig et al., 2020; Abhishek et al., 2022; Luo et al., 2023). These methods are all grounded in the data fusion process, deriving uncertainties for each water budget component from multiple data sources. Estimated uncertainties facilitate the determination of weights for allocating closure residuals, ultimately achieving a zero residual. Overall, these methods can be collectively referred to as data fusion-based closure correction approaches. Another recently developed method to constrain water balance employs an optimization-based strategy, exhibiting improved performance in long-term consistency with GRACE terrestrial water storage change (Petch et al., 2023). Other approaches, such as post-Processing Filtering technique (PF) and bias correction method (Munier et al., 2014; Weligamage et al., 2023), can also be helpful in closing water budget to ensure data consistency. However, the closure constraints imposed by the above methods (hereafter referred to as traditional methods) have been questioned, with Abolafia-Rosenzweig et al. (2020) arguing about the potential incorrect assignment of biases. If a component in the water budget exhibits a bias, closure correction algorithms may mistakenly apply the bias closure constraint to other components. The intrinsic attribution of this issue lies in the algorithms neglecting the physical correlations among components and imposing strict constraints on water budget closure by integrating uncertainties from multisource data. Or in other words, assigning closure residuals exclusively based on the magnitude of data uncertainty, without accounting for the distribution of components in hydrological processes, such as the partitioning of precipitation, may be unrealistic and could lead to erroneous allocation of closure residuals. In the context of applying such closure constraint, it becomes evident that the precision of certain individual components may notably deteriorate, particularly when uncertainties are challenging to quantify.

As is well-known, hydrological models, whether data-driven or physics-based, aim primarily to characterize hydrological processes by accurately allocating water quantities among components such as precipitation, evaporation, runoff, and soil moisture. In abstract terms, hydrological models can be regarded as directed graphs of fluxes, with nodes representing state variables and edges symbolizing fluxes or transitions (Wang and Gupta, 2024). Such directed graph is computationally closed, indicating that hydrological models inherently exhibit the essential characteristic of water budget closure. A clear piece of evidence comes from the data consistency evaluation conducted by Penning De Vries et al. (2021), who found that the dataset from the same model (i.e., precipitation and evaporation from ERA5 coupled model) manifested a well-closed system. In this sense, hydrological models appear capable of guiding the allocation of closure residuals to enhance water budget closure. Another distinctive feature of hydrological models, known as error adaptability or calibration compensation capability, underscores their pivotal role as innovative solutions for addressing challenges in achieving water budget closure. The feature emphasizes that hydrological models can, to some extent, compensate for biases in model inputs, outputs and structure, allowing satisfactory performance even when the utilized datasets exhibit certain inaccuracies (Wang et al., 2023). This provides hydrological models with the potential to integrate forcing and evaluation datasets into a unified water balance system under the soft constraint paradigm.

Here we propose another critical question regarding achieving water budget closure: Is the terrestrial water budget described by Eq. (1) fully comprehensive? This issue came to our attention through a recent study by Gordon et al. (2022), who examined the widespread validity of the Closed Water Budget (CWB) hypothesis (i.e., formulated by Eq. (1)) across 114 highland catchments using multiple data sources. Surprisingly, their results revealed that the CWB hypothesis failed to hold in 75% to 100% of the catchments. They highlighted that such failure of the CWB hypothesis could propagate widely in hydrological inferences relying on it, potentially leading to erroneous conclusions. To provide a physical explanation for the invalidity of the CWB, they extended Eq. (1) by introducing an error term e and additional term G, as depicted in Eq. (2).

$$e + G = P - ET - R - \frac{\mathrm{d}TWS}{\mathrm{d}t}, \tag{2}$$

The term G accounts for the inter-basin groundwater fluxes that were not considered in the original formulation, while the term e addresses inconsistencies among the original datasets. Clearly, when applying the CWB hypothesis for data evaluation or correction, there is a tendency to prematurely assume the completeness of the applied formulas, potentially leading to significant biases in the final results. Furthermore, in practical application, besides groundwater, the Eq. (1) may inadvertently omit other water fluxes and storages. For instance, utilizing gravity changes observed by GRACE to estimate TWS may encompass inter-basin water transfers or irrigation, which can have substantial influence in studies conducted at relatively small scales (Lv et al., 2017). Partial observations of precipitation, evaporation and runoff can also introduce biases into this equation. To distinguish the omission from total water budget residuals among the original datasets, we further extend Eq. (2) to obtain the generalized form as follows:

$$Res = Res_i + Res_o = P - ET - R - \frac{\mathrm{d}TWS}{\mathrm{d}t}, \tag{3}$$

where Res is the total water budget residuals; Res_i is the inconsistency residuals, accounting for the fraction of water non-closure due to physical inconsistencies among the original datasets; Res_o is the omission residuals, explaining the fraction resulting from omitted fluxes and storages in the original equation. We assume that Eq. (3) offers a comprehensive description of the terrestrial water budget and can be examined using multisource datasets. This advancement, compared to previous studies, breaks down the sources of water budget residuals, offering guidance for data evaluation and correction.

Given the current increase in data availability but concerns over reliability, this study aims to address the following scientific questions through physical hydrological processes modelling: (a) How can the total water budget residuals be decomposed into inconsistency and omission residuals? (b) From a large-sample perspective, what are the distribution patterns of these residuals? (c) What strategies can be employed to achieve water budget closure through physical hydrological processes modelling while strengthening the physical coherence among datasets from different sources? By addressing these questions, we highlight the necessity for a comprehensive description of the water budget equation to effectively evaluate and correct water closure. Furthermore, we develop a multisource datasets correction framework based on decomposition of water budget residuals and multi-objective calibration within hydrological modeling. The presented framework, providing the capability to enhance the water budget closure and hydrological connections among multisource datasets, is applied to a large-sample basins dataset across CONUS.

The remainder of this paper is organized as follows. Sect. 2 describe the main datasets used in this research. Sect. 3 then details the methods for decomposing water budget residuals and the multisource data correction framework with a hydrological model. The results are presented and discussed in Sect. 4 and Sect. 5. Sect. 6 provides the main conclusions and outlook of this study.

2 Data

2.1 The CAMELS dataset

Motivated by Gupta's call for large sample hydrological studies to strike a balance between depth and breadth (Gupta et al., 2014), in this study, we attempt to carry out analysis on a widely used large sample dataset, i.e., the Catchment Attributes and Meteorology for Large-sample Studies (CAMELS) community dataset, developed by Newman et al. (2015) and Addor et al. (2017). This dataset encompasses daily forcing, hydrologic response, and basin attributes for 671 basins across the contiguous United States (CONUS), characterized by minimal human disturbance. Drawing upon this dataset, a substantial body of experimental studies have been conducted, covering model intercomparison, analyses of hydrological scale effects, evaluations of model performance metrics, parameter estimation and exploration of machine learning models (Knoben et al., 2020; Beven, 2023). Grounded in large sample inquiries, these studies systematically explore the prevalent heterogeneity from different perspectives, yielding more robust and widely applicable conclusions.

In the original work proposed CAMELS dataset by Newman et al. (2015), a widespread physical inconsistency behavior was observed, characterized by an imbalance between precipitation and runoff. In the spatial depiction within the Budyko framework, certain basins exhibited plotting points exceeding the water limit line, indicating a surplus of runoff relative to precipitation. They emphasized the necessity for corrections to be applied to datasets. For the aforementioned reasons, investigation of the decomposition and reconciliation of water budget residuals on the CAMELS dataset is both necessary and feasible. In practice, the in-situ streamflow data observed by USGS National Water Information System server was used. Considering the availability of data products, our analysis is conducted over a common overlapping period spanning from 1998 to 2010. During this period, eighteen basins with missing streamflow observations were excluded in advance. Figure 1 presents a regional profile and the detailed information on the excluded basins is provided in supplemental Table S1.

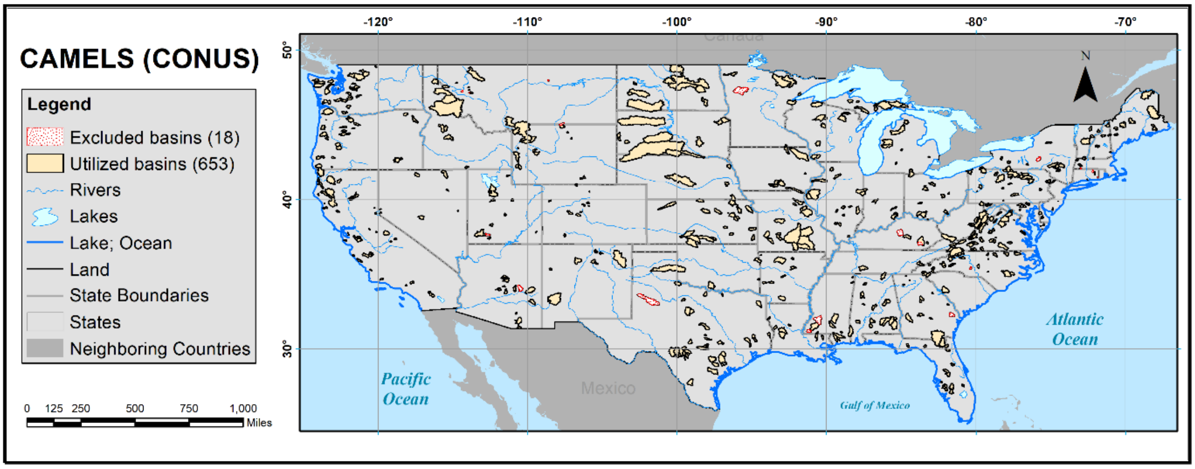

Figure 1. Geographic representation of the CAMELS Basins Dataset (Newman et al., 2015 and Addor et al., 2017). Eighteen basins excluded from the analysis are denoted by red dots, whereas the study incorporates the remaining 653 basins, emphasized with yellow shading. The copyright of the background map belongs to Esri (Gray Canvas Basemap).

2.2 Datasets for constructing water budget equation

The main aim of this study is to investigate the decomposition of water budget residuals and correction to datasets, rather than comparing the differences and rankings of closure residuals across different dataset combinations. In line with this objective, referring to the work of Petch et al. (2023), we strategically select single product for each water component to construct water budget equation, thereby laying the foundation for further research. In making this selection, we considered not only the resolution and spatiotemporal coverage of the products but also took into account recommendations from previous data evaluation studies regarding data accuracy (Kittel et al., 2018; Lehmann et al., 2022). All datasets used are summarized in Table 1.

Specifically, daily precipitation estimation derived from the Tropical Rainfall Measuring Mission (TRMM 3B42V7) is used in this study. For evaporation, we utilized the third version of Global Land Evaporation Amsterdam Model (GLEAM v3) product (https://www.gleam.eu/), which employs a set of algorithms to separately estimate the different components of land evaporation (Miralles et al., 2011). And, as mentioned above, the runoff measurements on a basin scale are provided by the CAMELS dataset. Finally, the most challenging component to estimate in the water budget equation is the Terrestrial Water Storage Change (TWSC) as it includes water both on and below the Earth's surface. In the previous studies, the measurement of gravity field changes, as provided by the Gravity Recovery And Climate Experiment (GRACE) product, has been frequently employed for the estimation of the TWSC (Luo et al., 2020; Kabir et al., 2022). This approximation is based on the assumption that, for a given large-scale basin, variations in mass are primarily attributed to changes in TWSC. However, the assumption is fragile when applied to small basin, leading to significant uncertainty in estimating TWSC for basins with areas less than 63,000 km2 (Lehmann et al., 2022). This study focuses on the basins dataset from the CAMELS, with most basin areas being smaller than this threshold. To avoid introducing additional uncertainty into the analysis, we need alternative methods to estimate TWSC.

Assuming that TWSC can be retrieved through a combination of different water storages, we obtained the four-layer soil moisture from ERA5 Land and Snow Water Equivalent (SWE) from GlobSnow to estimate overall TWSC. This approach has been implemented in the investigation of Hoeltgebaum and Dias (2023), yield a high consistency between estimated TWSC and GRACE observation (i.e., correlation coefficient exceeding 0.71). Another consideration in this method is that the decomposed TWSC products (i.e., soil moisture and SWE) can correspond to the results simulated by hydrological model, thereby allowing us to correct water budget residuals, as discussed later.

Overall, all datasets were resampled to a daily time step, and then aggregated over basins through simple averaging to perform analysis of water budget closure on a basin scale. Including the observed runoff from CAMELS, all data were converted to water depth (mm) to construct a unified water budget equation. It is noteworthy that there are certain missing data in GlobSnow SWE varying across basins. To fill these data gaps, we set a window of length 5 centred on missing data. We applied linear interpolation within the window for gap filling. If linear interpolation was not feasible due to, for instance, the absence of valid values within the window, mean climatology was employed to fill the missing data. To illustrate this, we randomly selected nine basins and visually depicted the gap filling process in supplemental Fig. S1.

Table 1. Overview of the products for constructing water balance equation used in this study.

Variable	Product	Original Resolution		Period	Reference
		Spatial	Temporal		
Precipitation	TRMM 3B42V7	0.25°×0.25°	Daily	1998-2019	*Huffman et al. (2016)*
Evaporation	GLEAM v3.8a	0.25°×0.25°	Daily	1980-2022	*Martens et al. (2017)*
Soil moisture layer 1/2/3/4	EAR5 Land	0.1°×0.1°	Hourly	1950-present	*Muñoz Sabater et al. (2021)*
Snow water equivalent	GlobSnow v3.0	25km×25km	Daily	1979-2018	*Luojus et al. (2021)*

3 Methods

To leverage physical hydrological processes modelling for the decomposition and correction of water budget residuals, the following assumptions are necessary: (1) the hydrological model provides a reliable representation of hydrological processes, ensuring an accurate partitioning of input precipitation; (2) the uncertainties associated with the model forcing and structure can be considered negligible during the modelling process. These two hypotheses form the foundation of this work. To ensure the validity of Hypothesis 1, we employed multiple evaluation variables and corresponding metrics to guarantee the overall reliability of the model, which will be detailed in the model setup section. Additionally, it is pertinent to acknowledge the Hypothesis 2 represents a strong assumption, carrying inherent uncertainties. Despite this, it is necessary for the feasibility of the overall work, and we will further explore the influence of this hypothesis on the results in the discussion section.

3.1 Decomposition of water budget residuals: inconsistency and omission residuals

Our strategy for decomposing water budget residuals is grounded in the computational closure of the hydrological model. As previously discussed, conceptualized as a directed graph, the difference between inputs and outputs of the model must necessarily equal to the change in state variables. Stated differently, there is a water balance between the forcing and simulated variables of the model, with no physical inconsistency residuals present. Therefore, setting the inconsistency residuals in Eq. (3) to zero allows us to derive the water budget equation of the hydrological model as follows:

$$Res_o = P_{forcing} - ET_{sim} - R_{sim} - \frac{\mathrm{d}TWS_{sim}}{\mathrm{d}t}, \tag{4}$$

where the subscripts "forcing" and "sim" denote the forcing and simulation values, respectively. Simultaneously, integrating the multisource datasets described in Sect. 2.2 into Eq. (3) yields the total water budget residuals (i.e., Res). For convenience, we refer to the water budget characterized by the hydrological model as the simulation system and the one constructed by multisource datasets as the measurement system. When the hydrological model calibrated against multiple variables measured by the multisource datasets and achieves reliable performance, we consider the simulation system approaching the measurement system. At this point, the difference between Eq. (3) and (4) represents the omission residuals (i.e., $Res_i = Res - Res_o$), indicating the water fluxes or storages omitted by the original equation. Thus, the total water budget residuals can be decomposed into inconsistency and omission residuals. It is noteworthy that while the inconsistency residuals are absent in the simulation system—a physical consistent system—omission residuals may still exist due to inherent omissions in the original equation. Hence, the left-hand side of the Eq. (4) may not be zero.

Considering the comparability of available datasets and model simulations, we have developed more specific expressions for Eq. (3) and (4), as depicted below.

$$Res = Res_i + Res_o = P_{TRMM} - ET_{GLEAM} - R_{USGS} - \frac{\mathrm{d}SWE_{GlobSnow} + \mathrm{d}SM_{ERA5}^{0\sim 50cm} + \mathrm{d}SM_{ERA5}^{50\sim 289cm}}{\mathrm{d}t}, \tag{5}$$

$$Res = Res_o = P_{TRMM} - ET_{sim} - R_{sim} - \frac{\mathrm{d}SWE_{sim} + \mathrm{d}SMS_{sim} + \mathrm{d}GRS_{sim}}{\mathrm{d}t}, \tag{6}$$

where the subscripts indicate variable sources, such as measurements and simulated values, and superscripts for SM denote the depth of soil layers to be aggregated. The above water budget equations are discretized employing a simple central difference scheme with a two-day time step at the daily scale (Petch et al., 2023).

https://doi.org/10.5194/hess-2024-230
Preprint. Discussion started: 5 August 2024

It is important to further clarify that the hydrological model used in this study (see below) divides total soil moisture into soil water storage (SMS_{sim}, hereafter SMS) and groundwater reservoir storage (GRS_{sim}, hereafter GRS). The soil moisture measurements, ERA5, on the other hand, employs the H-TESSEL (Hydrology Tiled ECMWF Scheme for Surface Exchanges over Land) land surface scheme to characterize land surface hydrological processes (Balsamo et al., 2009), dividing soil into four layers (i.e., 0~7 cm, 7~28 cm, 28~100 cm and 100~289 cm). In the H-TESSEL model, the upper 50 cm of soil column is defined as the effective depth for generating surface runoff. To ensure consistency between the simulation and measurement systems, we match the top 50 cm of ERA5 soil moisture with the soil water storage in the hydrological model, while the depth range of 50 cm to 289 cm corresponds to the groundwater reservoir storage in the hydrological model.

3.2 Multisource datasets correction framework for achieving water budget closure

Here, we introduce an innovative Multisource Datasets Correction Framework grounded in Physical Hydrological Processes Modelling to enhance water budget closure, termed PHPM-MDCF. Unlike traditional correction methods that use uncertainty (typically derived from the variance of multisource datasets for the same variable or priori estimation) as a weight for allocating water budget residuals, this framework leverages the hydrological model—a physical consistent system—as a constraint to correct the measurement system. Figure 2 indicates the flowchart for the correction framework and the procedure is described as follows:

- Step 1: Initialize the basic computing unit. Calibrate hydrological model, calculate the total water budget residuals from the original datasets, and then decompose them into inconsistency and omission residuals following the method outlined in Sect. 3.1. This step is denoted as iteration 0.
- Step 2: Correction for the inconsistency residuals. Allocate inconsistency residuals based on the magnitude of differences (i.e., the distance between simulation and measurement systems) between simulated and measured values for each variable in Eq. (5) and (6). Here, an initial correction rate of 0.5 is set to gradually correct the multisource datasets, thereby avoiding potential uncertainties that arise from excessive correction.
- Step 3: Calibration and evaluation of the model. Recalibrate and evaluate the hydrological model using the datasets corrected in the previous step to assess the reliability of this correction. If the recalibrated model yields unreliable simulations, consider this correction excessive, halve the correction rate, and repeat Step 2. Otherwise, maintain the correction rate and proceed with the next iteration of correction.
- Step 4: Iteration and termination of correction. Iterate through Steps 2-3 to gradually correct the datasets until the inconsistency residuals decreases to 10% of its initial value or the correction rate falls below 4%.

The design goal of the PHPM-MDCF is to impose soft constraint on multisource datasets through the calibration compensation capability and the physical consistency feature of the hydrological model. Such a constraint is referred to as “soft” because, unlike traditional methods that import “hard” constraints, the correction process does not strictly require residuals to be zero

immediately. Instead, it aims to advance the convergence between the simulation and measurement systems, as illustrated in
270 Fig. 3. The efficiency of ultimately closing residuals depends on the ability of model to accurately characterize real world, and this can vary across different locations.

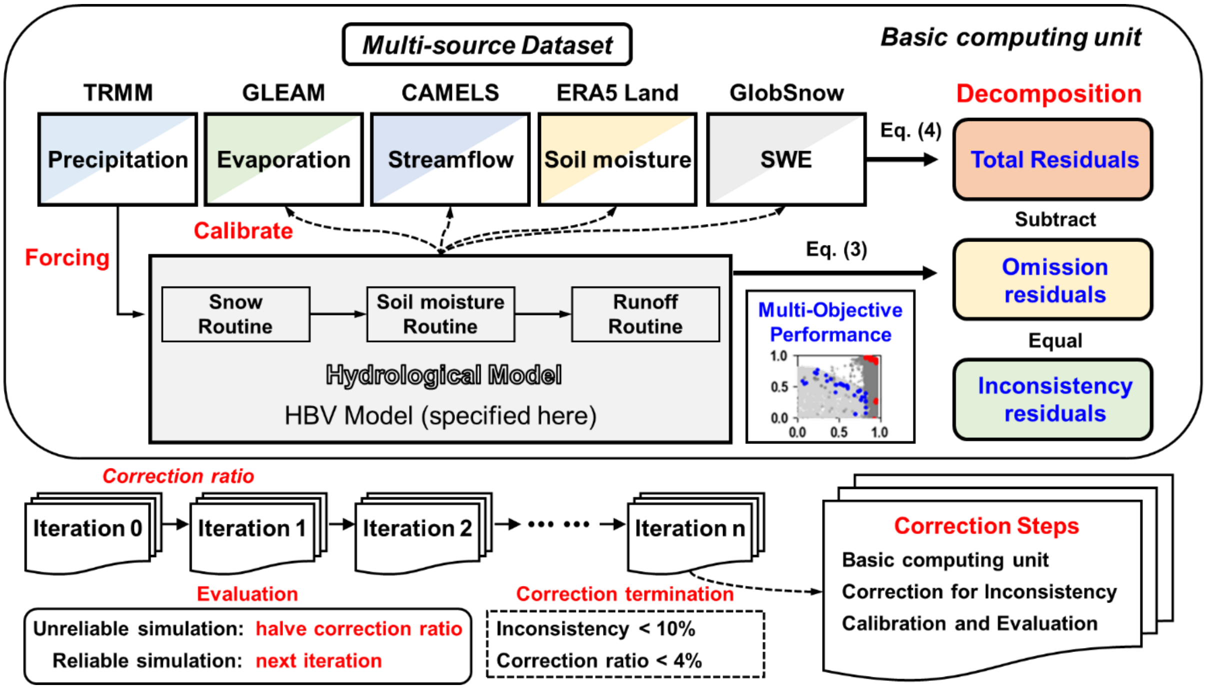

Figure 2. Flowchart of the multisource datasets correction framework grounded in physical hydrological processes modelling, PHPM-MDCF.

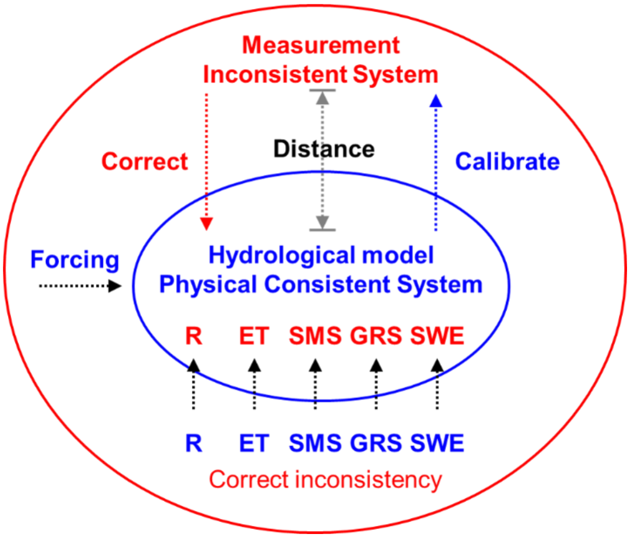

Figure 3. Illustration of the correction process advancing convergence between the simulation and measurement systems.

3.3 Model setup and calibration

In the present investigation, we employed the Hydrologiska Byråns Vattenbalansavdelning (HBV) model, to implement our correction framework. The conceptual HBV model was developed by the Swedish Meteorological and Hydrological Institute (SMHI) in the 1970s (Bergström, 1976). Given its straightforward yet effective design and minimal input requirements, this model has attained broad recognition and application within the global hydrological modelling scientific community, which has also been tested in the CAMELS basins (Feng et al., 2022). Here we provide brief details and refer the reader to the above references for a fuller description.

The basic structure of the HBV model comprises three main modules: the snow routine, soil moisture routine, and runoff routine, as illustrated in Fig. A1. Starting with precipitation forcing, water flux traverses through the three modules, accumulating in various state variables such as snow and soil water. Ultimately, water is released through three reservoirs—soil moisture, upper zone, and lower zone reservoirs—as quick runoff, interflow, and base flow. Thus, the overall soil moisture can be divided into soil water storage (i.e., the first reservoir) and groundwater reservoir storage (i.e., the combination of the latter two reservoirs). In the current study, the HBV model is configured to run of a daily basis, aligning with both the forcing and evaluation datasets, ensuring the feasibility of subsequent correction. Table A1 lists the free parameters slated for calibration in the HBV model, providing their descriptions and respective ranges.

Here, a multi-objective global optimization algorithm, the Non-dominated Sorting Genetic Algorithm II (NSGA-II), is applied for parameter calibration of the HBV model. Owing to its optimization efficiency, this algorithm has been extensively used in hydrological modelling practices around the world (Mostafaie et al., 2018). For more details about the algorithm, see Deb et al. (2002). We implemented the calibration framework using the NSGA-II algorithm in a Python environment with the DEAP package (Fortin et al., 2012). Five calibration objectives are considered, including R (runoff), ET (evaporation), SMS (soil moisture storage), GRS (groundwater reservoir storage) and SWE (snow water equivalent). Meanwhile, the Kling-Gupta Efficiency (KGE) metric (Gupta et al., 2009) is utilized to evaluate the simulation performance of R and ET, while the Pearson correlation coefficients (r) is employed to evaluate the performance of SMS and GRS, considering potential discrepancies in their magnitudes arising from differences in soil layer depth. Finally, the Root Mean Square Error (RMSE) is applied to evaluate the simulation performance of SWE. Ideally, the optimal simulation is characterized by values of 1 for the first two metrics and 0 for the last one. The detailed description of the evaluation metrics is provided in Appendix B.

4 Result

4.1 Distribution of water budget residuals and its components across the CAMELS basins

In this section, we investigate the spatiotemporal distribution of water budget residuals for each component decomposed using the method proposed in Sect. 3.1 across the large sample of CAMELS basins. This result provides insights into the two primary sources of non-closure issue in water budget equation—physical inconsistencies among the original datasets and water fluxes or storage omitted in the original equation. To ensure the robustness of the results, as mentioned previously, it is essential that hydrological model reliably represent hydrological processes. With reference to previous studies (Clark et al., 2021), we have adopted KGE ≥ -0.41 and r statistically significant at the 5% level as criteria for guaranteeing reliable simulations. The multi-objective simulation performances of the HBV model are detailed in Appendix C. In general, the majority of basins (475, accounting for 72.24% of the total basins) achieved reliable simulations across all variables. Among them, we have observed that the central and western CONUS present relatively greater challenges for modelling. This pattern and its potential causes will be further explored in the ensuing discussion.

Within the 475 basins demonstrating reliable simulations, in Fig. 4 we plotted the spatial distribution of the long-term monthly mean water budget residuals (Res), inconsistency residuals (Res_i), and omission residuals (Res_o). An important observation from comparing different rows of Fig.4 is that Res shares a similar spatial pattern with Res_i, whereas Res_o exhibits some differences. This pattern exists across different quantile ranges of the residuals. For instance, Res and Res_i both present an east-west gradient for three statistical measures (i.e., min, median, max), with low values occur along the western coastline and high values primarily concentrated in eastern inland basins. The exception is a cluster of low median values located in the central CONUS. Interestingly, the minimum values of Res_o display a contrasting spatial pattern, with higher values in the west and lower values in the east. The spatial difference in median and maximum values of Res_o are not pronounced. These patterns lend support to the underlying assumption that the drivers of inconsistency residuals and omission residuals are fundamentally different, and thus can be decomposed from the total water budget residuals.

https://doi.org/10.5194/hess-2024-230
Preprint. Discussion started: 5 August 2024

Figure 5 further illustrates the temporal distribution patterns of the three residuals in terms of seasonality. It is readily 330 discernible in the figure that the similarity between Res and Res_i reappears, manifesting distinct seasonal patterns with more pronounced negative trends during the cold seasons (i.e., October to the following April) and positive trends during warm seasons (i.e., May to September). On the contrary, Res_o tends to be mainly positive except from September to November; its extent of variability is also significantly smaller than that of the other two residuals (Fig. 5c). In regard to magnitude, Res_i is greater than Res_o, whether considering positive or negative bias (Fig. 5d-f). From the above results, we can conclude that Res_i 335 predominates within Res, exhibiting significant spatiotemporal difference from Res_o. These two residuals may combine or offset each other to collectively form the total water budget residuals.

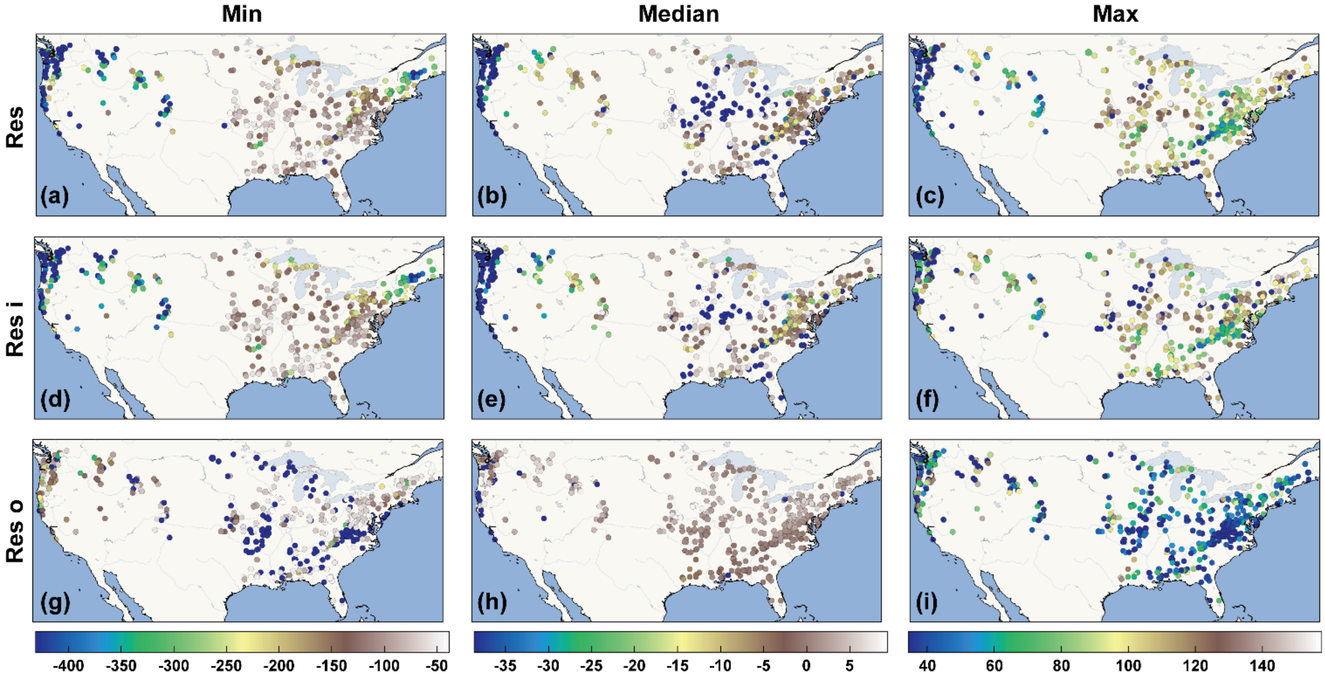

Figure 4. Spatial distribution of long-term monthly mean water budget residuals (Res), inconsistency residuals (Res_i), and omission residuals (Res_o) across 475 CAMELS basins with reliable simulations. The unit of residuals is "mm".

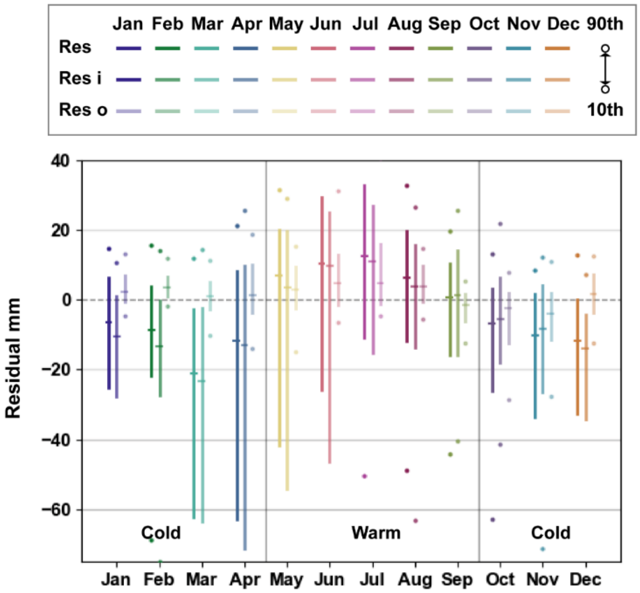

Figure 5. Temporal distribution of monthly water budget residuals (Res), inconsistency residuals (Res_i), and omission residuals (Res_o) across 475 CAMELS basins with reliable simulations. (a-c) Boxplots describe variability across seasons; (d-f) Time series of residuals and their quantiles (i.e., 50th, 10-90th, 25-75th), along with the grey scatters corresponding to various basins. The unit of residuals is "mm".

4.2 Efficiency of the PHPM-MDCF

We are now tackling the third question through the proposed multisource datasets correction framework (PHPM-MDCF) across the 475 CAMELS basins with reliable simulations. For illustration, several case basins have been selected to demonstrate the correction process and its efficiency.

Figure 6 shows the correction results at the case basin numbered 1013500 (for more details about the basin number, see Newman et al. (2015)). As expected, the time series of Res and Res_i after correction (red lines) tend to be flatter compared to their uncorrected counterparts (blue lines). This becomes more apparent as the timescale increases. However, despite recalibrating the model with corrected datasets, Res_o driven by the omission in water budget equation exhibited no substantial changes before and after correction (e.g., the monthly mean absolute values maintain around 6.5 mm, see Fig 6f). This phenomenon occurs because we only corrected the inconsistency residuals with reference to the simulation system, while the omission accounting for addition water terms should not be corrected in the existing datasets. This result also indicates the robustness of the decomposition and correction method, as they do not significantly change the identified omission residuals.

To get an impression of the PHPM-MDCF correcting water budget residuals, the bottom row of Fig. 6 shows the variation of mean absolute values of three residuals with increasing correction iterations at the monthly scale. The results indicated that the correction process led to a significantly reduction in Res and Res_i, decreasing from 42.8 mm and 44.3 mm to 6.9 and 8.6 mm (approximately 83.9% and 80.7% reduction). Although water budget residuals cannot be fully corrected to zero in this framework (as they do in traditional methods), we argue that this correction efficiency is satisfactory enough. It is rooted in physical hydrological process modelling, thus potentially strengthening the physical relationships among the components of the water balance. The final corrected result for this case basin are presented in Fig. S2, depicting the time series of multisource datasets before and after correction. In the following sections, we will provide further evidence of the credibility of this correction framework.

The correction results for several other case basins (i.e., numbered as 1137500, 2177000, 6311000 and 14092750) are presented in Fig. S3-6. Their absolute mean monthly residuals decreased by 70.4%, 58.1%, 40.3%, and 54.0%, respectively, providing evidence for the effectiveness of the PHPM-MDCF. To have a clearer idea of the ability of the correction framework to reduce water budget residuals across all the CAMELS basins, Fig. 7 shows the map of the percentage reduction in monthly total water budget residuals after corrections. In general, the PHPM-MDCF demonstrated robust performance across most basins, with an averaged reduction percentage of 49% across all basins. The correction efficiency exhibits a latitudinal-dependent decline pattern, which primarily due to the small initial residuals in low latitude regions (Fig. 4). In high-latitude regions, such as the western coastline and eastern inland basins mentioned earlier, the potential correction space is much larger, leading to higher correction efficiency (in terms of absolute value).

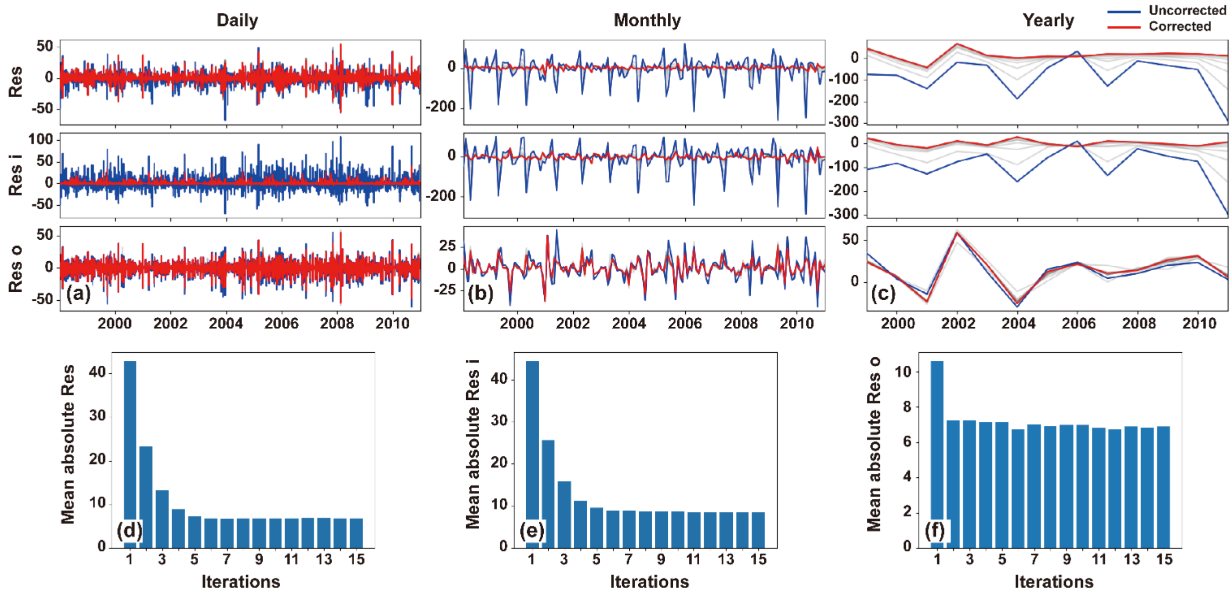

Figure 6. Correction results of water budget residuals for multisource datasets at basin 1013500. (a-c) Time series of water budget residuals (Res), inconsistency residuals (Res_i), and omission residuals (Res_o) at daily, monthly and yearly scales, grey line represents residuals during the correction process. (d-f) Variation of long-term mean absolute values of three residuals with correction iterations at the monthly scale. The unit of residuals is “mm”.

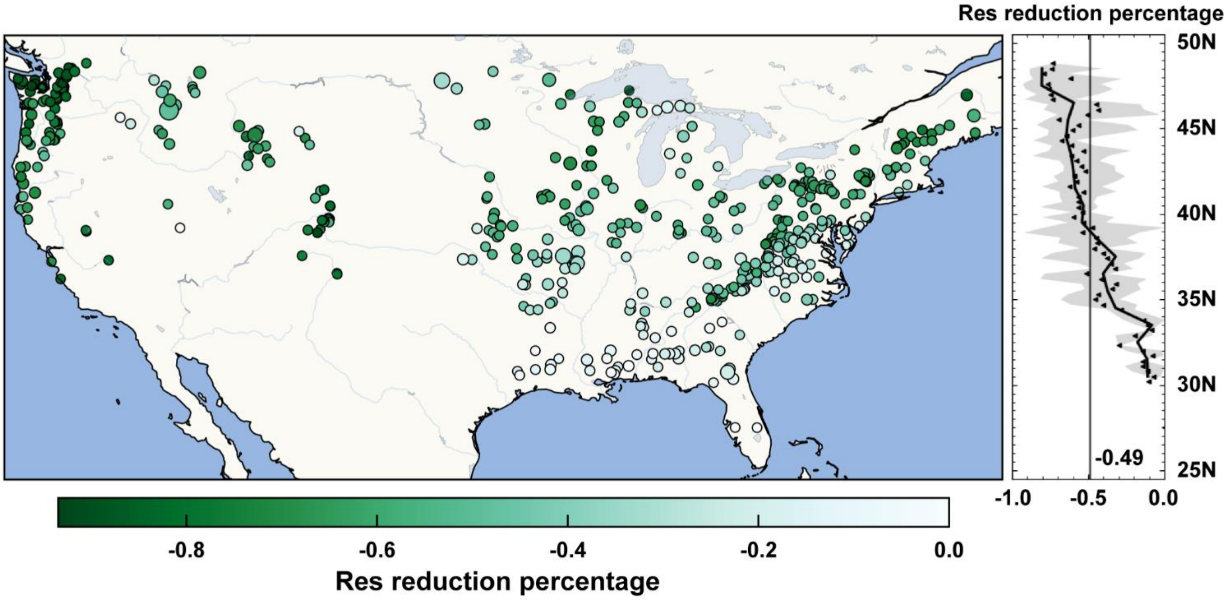

Figure 7. The percentage reduction of monthly total water budget residuals after correction through the PHPM-MDCF. Zonal means (right panel) include mean (black scatters), median (black line) and range (gray shading). The vertical line indicates the mean of all basins.

4.3 Credibility of multisource datasets correction

4.3.1 Convergence between simulation and measurement system

As we stated before, the core objective of the PHPM-MDCF is to promote the convergence between the simulation and measurement systems (Fig. 3). In fact, this process can be divided into two parts. The first part, namely the measurement system approaching the simulation system, which is implemented by correction procedures, has gained confidence from the significant reduction in the inconsistency residuals (Fig. 6). On the other hand, to illustrate the convergence of the simulation system towards the measurement system, we present the changes in model simulation performance before and after correction of case basin 1013500, as depicted in Fig. 8. From the figure, we can clearly see that both the population solution sets (ranging from light to darker grey scatters) and the Pareto fronts (ranging from blue to red scatters) tend to the optimal point at the upper right corner after correction. This suggests that the PHPM-MDCF has the ability to enhance hydrological model performance at specific locations without changing the forcing. Meanwhile, this result also provides evidence of the convergence between the simulation and measurement systems within the correction framework, supporting the credibility of the correction results to some extent.

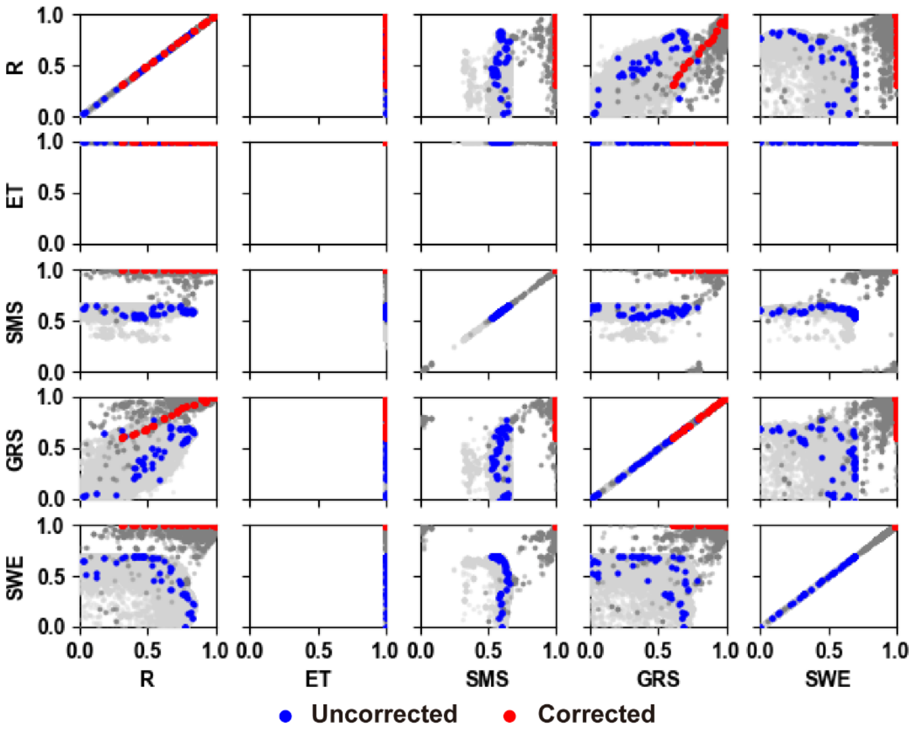

Figure 8. Comparison of multivariable simulation performance before and after correction at basin 1013500. Light grey and dark grey indicate population solution sets before and after correction, and blue and red indicate Pareto fronts before and after correction. Metrics evaluating SWE simulation performance have been normalized for consistency.

4.3.2 Noise experiments

To further demonstrate the credibility of multisource datasets correction, we designed a series of noise experiments and applied them to the case basin 1013500, therefore examining whether the PHPM-MDCF can effectively handle the manual noises and produce robust correction results. These experiments are summarized in Table 2, where the first three experiments set different types of single-point noise at different positions of the same original datasets, and the last experiment adds an equal-length Gaussian white noise sequence to the runoff sequence. Eventually, two new noisy datasets were generated, as illustrated in Fig. S7 and S8. For clarity, we refer to them as NS1 (i.e., noise sequence) and NS2, and designate the noise-free datasets as OS (i.e., original sequence). The noise points are ordered from 1 to 4.

First, we examined the adaptation capability of the PHPM-MDCF to single-point extreme errors. The top row of Fig. 9 compares the differential forms of the OS and NS1, highlighting the impact of the three noises. The first two noises introduce extremely unreasonable values in the runoff measurements, while the third noise significantly affects water balance by altering all water budget variables, as evidenced in Fig. 9c-d. Through the application of the PHPM-MDCF for NS1 correction, we

https://doi.org/10.5194/hess-2024-230
Preprint. Discussion started: 5 August 2024

derived a new corrected sequence and compared it with the previous OS-based corrected sequence. In terms of runoff correction, as shown in Fig. 9c, whether extreme large or small noises (i.e., noise 1 and 2 with differences of three standard deviations), the correction process constrains them to reasonable runoff processes. This is achieved by the representation of physical hydrological processes underlying the correction strategy, implemented in the hydrological model, such as runoff generation and routing. Furthermore, water imbalance caused by combination of multivariable single-point noises can also be constrained to minimal levels through correction (Fig. 9d).

Another concern here is whether the correction of extreme noises in runoff will propagate to other variables, potentially leading to a series of unreasonable correction results, as questioned by Abolafia-Rosenzweig et al. (2020) regarding traditional methods. In Fig. S9, we specifically focus on the correction results around three single-point noises to address this question. The fact that simultaneous corrections of other variables during extreme runoff noises correction did not significantly alter compared to OS-based corrections further enhances our confidence in PHPM-MDCF. It suggests that the soft constraints based on physical hydrological processes will not lead to compensatory errors, as seen in traditional methods due to the rigid allocation of water budget residuals.

Subsequently, we assessed the robustness of correction results after incorporating Gaussian white noise into the original sequence. From the comparison between OS-based and NS2-based correction results (Fig. 10), it can be seen that the addition of Gaussian white noise slightly changes the correction in runoff, such as a minor decrease in the high-value range (with a slope less than 1). However, the overall evolution trend of runoff remains unchanged, as it is still constrained by the same hydrological physical processes. In such a basis, as excepted, the correction of other variables is minimally affected by Gaussian white noise in runoff.

In summary, the results yield from the above experiments indicate that both single-point noise and Gaussian white noise have minimal impact on the corrections. The final correction results are constrained by the hydrological model, with random errors in measurements not significantly altering the allocation of water budget residuals. The physical relationships among various water budget variables, as representation by the model, are also imposed onto the measurements through the correction process. This constitutes the core principle of PHPM-MDCF.

Table 2. Description of the noise experiments to examine the credibility of multisource datasets correction.

ID	Description	Position of the noises	Noise sequence
Exp. 1	A single positive-biased noise is added to R, with a magnitude of three standard deviations	Noise1: 1998-09-18	NS1
Exp. 2	A single negative-biased noise is added to R, with a magnitude of three standard deviations	Noise2: 1999-04-26	

Exp. 3	A set of positive-biased noise at the same position are added to R, ET, SMS, GRS, and SWE, with a magnitudes of one standard deviation	Noise3: 2001-12-16	
Exp. 4	A series of zero-mean random Gaussian white noise is added to R, with a standard deviation of 20% relative to the original sequence	Noise4: the entire sequence	NS2

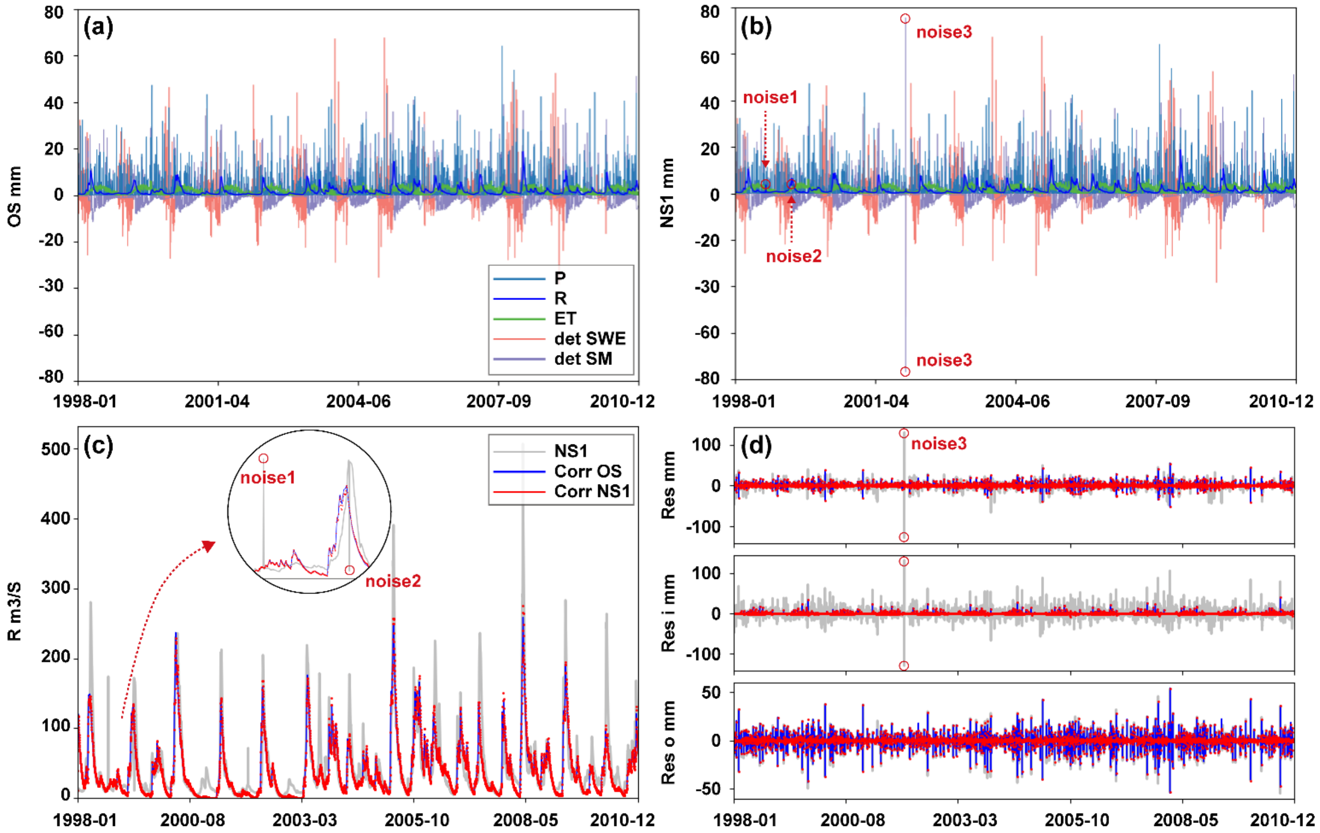

Figure 9. Correction results for multisource datasets corresponding to noise experiments 1-3. (a-b) Time series of OS and NS1 in form of differences. (c) Comparison among the runoff noise sequence (NS1), OS-based runoff corrected sequence (Corr OS), and NS1-based runoff corrected sequence (Corr NS1). (d) Comparison of water budget residuals generated by the three sequences at daily scale.

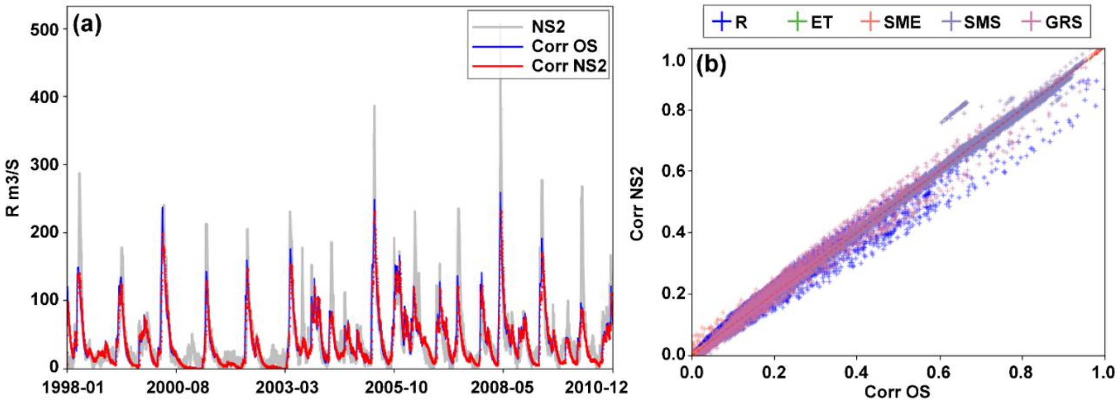

Figure 10. Correction results for multisource datasets corresponding to noise experiments 4. (a) Comparison among the runoff noise sequence (NS2), OS-based runoff corrected sequence (Corr OS), and NS2-based runoff corrected sequence (Corr NS2). (b) Comparison of multivariable between OS-based correction and NS2-based correction in terms of standardized values.

4.4 Potential influencing factors of water budget residuals

In this section, we conducted a preliminary exploration of the potential factors influencing the formation and distribution of water budget residuals. As shown in Fig. 4, all three water budget residuals are subject to strong spatial organization, and these patterns are in agreement with previous studies. For example, Kauffeldt et al. (2013) found negative residuals (i.e., runoff coefficient > 1) along the western coastline of CONUS, while the eastern region showed notable positive residuals (i.e., P-R > ET). Other studies investigating water budget residuals with diverse dataset combinations have similarly revealed similar spatial patterns (Zhang et al., 2016; Gordon et al., 2022). Therefore, we speculate that the closure of water budget is predominantly influenced by the characteristics of the basin.

Here we focus on the total water budget residuals (i.e., Res) and attempt to relate it with the hydro-meteorological conditions and the basin area. To bring out these relationships, from Fig. 11, three regression curves are obtained by correlating mean absolute residuals at different timescale with basin areas over 475 CAMELS basins. The negative gradients of the curves imply that as basin area increases, the water balance constructed from multisource datasets can be enhanced. In other words, special attention should be paid to testing the assumption of water budget closure when employing multisource datasets for hydrological inferences in small basins, thereby mitigating potential issues of physical inconsistency.

Moreover, as expected, hydro-meteorological conditions within the basin play a crucial role in controlling the distribution of water budget residuals. The clear delineation between different levels of daily precipitation and runoff coefficient revealed in Fig. 11 strongly supports this reasoning, where multisource datasets yield larger water budget residuals in basins with high precipitation and runoff coefficients—large red spots are located in the upper portion of the figure. An additional investigation to provide more detailed attribution of water budget residuals distribution with more basin characteristics is a valuable research topic, but it requires substantial work beyond the scope of this study. We fully expect that increased attention will be directed toward this topic in the future, which will enhance the understanding of water budget non-closure issue in related disciplines.

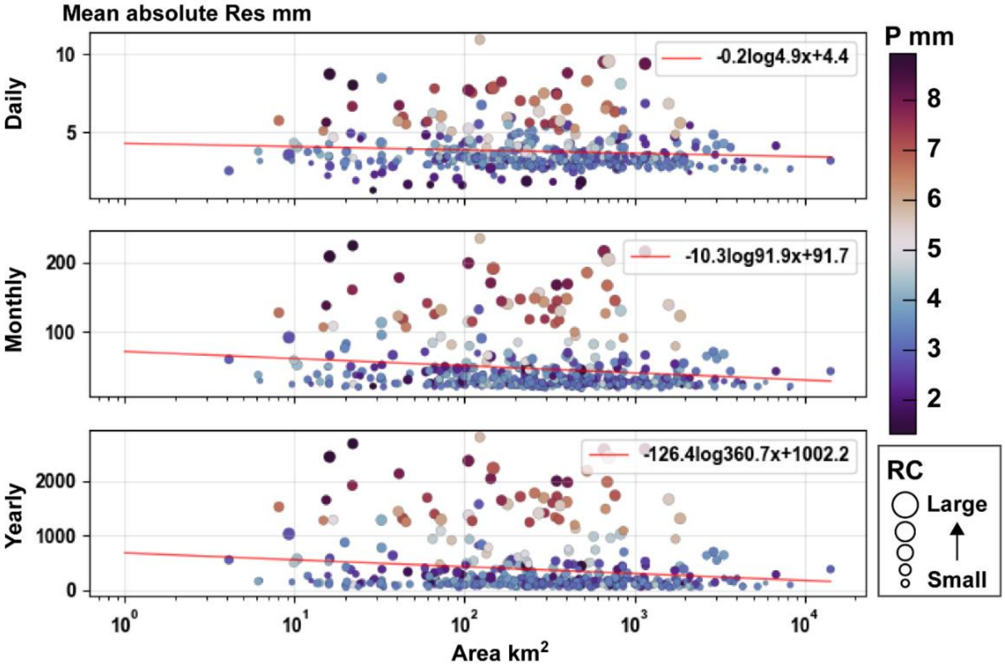

Figure 11. Relationship between the mean absolute of water budget residuals, basin area, long-term average daily precipitation, and runoff coefficient (RC) over 475 CAMELS basins with reliable simulations. The respective red lines represent the linear regression of residuals with basin area for each timescale.

5 Discussion

5.1 What Lies Within the Realm of Belief

The foundation of modern experimental science is based on empiricism, emphasizing the repeatability of experiments, i.e., whether the results can perfectly reproduce observations. This idea has far-reaching implications across various fields, with a classic example being hydrologists always aiming for their model predictions to closely match observations. Importantly, the underlying assumption of this approach is that our observations are perfectly approximate reality and can be seen as true value. In most of small scale studies, such as those conducted in laboratory or field settings, this might hold true. However, as we shift our focus to larger spatial scales, obtaining observations directly often becomes challenging, thus necessitating reliance on indirect observations, which could potentially undermine this assumption. As a consequence, our confidence in the observations, or better referred to as measurements, may diminish, which is precisely the new challenge we face in the era of big data.

When we lack sufficient confidence in any single measurement, the utilization of multisource data fusion becomes a method to mitigate errors from all sources of measurements, thereby reducing uncertainty. Within the process of data fusion, the basic step is to determinate the weights of all components. The ensemble mean method assumes an equal weight for all components, while the simple weighted method estimates weights based on the priori uncertainties, which are typically the differences between each component and the average of all measurements (Sahoo et al., 2011). In the widely used triple collocation (TC) method, weights can be determined by calculating errors (uncertainties) based on the similarity of the triplet inputs, without the need for "ground truth" (Stoffelen, 1998). Some other methods also determine uncertainty through manually assigned constants or error propagation calculations (Munier et al., 2014; Ansari et al., 2022). However, all of these methods face the same issue, the true value may be unattainable, and the determined error or uncertainty involves subjective factors. This presents a logical paradox: we resort to data fusion due to the absence of a true value, yet during the fusion process, we paradoxically assume the existence of this true value to estimate uncertainty. Essentially, we need to answer a fundamental question: what do we truly believe in?

The answer is what we have truly learned. A better approach is to leverage our existing knowledge about the physical world to enhance our confidence in measurements. In fact, this concept embodies to some extent a Bayesian philosophy and is reflected in many fields. Here, we present two modern examples to illustrate this idea. The first one is the atmospheric reanalysis, which has been one of the most significant topics in atmospheric science since the 19th century. This technique employs numerical models and assimilation techniques to integrate multiple types of historical measurements a unified modelling framework and assimilation scheme, thereby generating continuous and consistent estimates of climate states. In essence, its aim is to unify our knowledge system (i.e., numerical models) with the measurement system, thereby enhancing the credibility of the model output.

Another example is a research in the field of hydrology, where Liao and Barros (2022) proposed an Inverse Rainfall Correction (IRC) framework to improve Quantitative Precipitation Estimates (QPE) in headwater basins. Their fundamental concept is that errors propagate from precipitation to runoff, enabling the reversal of precipitation errors by calculating runoff simulation errors from distributed hydrological models and applying the travel time distribution for correction. In this example, existing knowledge is represented by the hydrological model, which is assumed to reflect the true physical processes and is then used to enhance the confidence in precipitation measurements. Although our current knowledge may not be entirely precise—for example, the depiction of hydrological processes in hydrological models may lack accuracy—it remains foundation upon which we can rely and strive to refine in the future.

The proposed correction framework (PHPM-MDCF) capitalizes on this concept by iteratively advancing the convergence between the knowledge system (i.e., hydrological model and water balance equation) and the measurement system, thus enhancing the credibility of the measurements. The underlying concepts in this framework, such as residuals decomposition and advancing water budget closure through correction, is align with a recent study (Wang and Gupta, 2024). Specifically, they introduced a novel hybrid model (i.e., Mass-Conserving-Perceptron) and discussed its potential application, including the bias correction (lacking confidence for the measurements) and examination of non-observed interactions with the environment (corresponding to the omission errors). Coupling the hybrid model with PHPM-MDCF to replace the hydrological model seems to be an interesting avenue for future development and research.

5.2 Limitations and Paths Forward

It is our opinion that some traditional hydrological inferences are based on a philosophy that involves some long-standing and problematic assumption arise from the unwarranted confidence in measurements. However, the fact that truth is almost impossible to be measured due to the complexity of real-world physical processes hampers the foundation of inferences, especially in large scale studies that employing multisource non-field data. The presented framework has advantages by integrating widely applicable water budget equation and reliable representation of hydrological process using a hydrological model, which significantly mitigates this issue and enhance our confidence to the corrected datasets. Although the efficiency and credibility of the PHPM-MDCF have been examined in the previous sections, there are several limitations and uncertainties worthy of further discussion.

5.2.1 Uncertainty of forcing data

Here, we return to the Hypothesis 2 posed at the beginning of the method section. As we acknowledge, the uncertainties arising from the forcing and model structure undeniably exist and were a limitation in this study. To investigate the sensitivity of correction results to forcing data, we re-conducted multisource datasets correction using Daymet precipitation data at the same case basin (1013500) and compared it with the original correction (forcing by TRMM). The top panels of Fig. 12 display slight differences between the two corrections; for instance, the Daymet correction shows lager SWE (with a slope greater than 1), while other variables are smaller. These differences can be entirely explained by variations in precipitation forcing. Nevertheless, the temporal patterns of all variables under the two corrections remain broadly consistent, with slopes of all regression curves exceeding 0.85 (Fig. 12b). This emphasizes the constraining role of the hydrological model within the correction framework, and also reflects the adaptability of the model to input errors.

Another evidence of the robustness of the PHPM-MDCF is provided by Fig. 12c-d, where corrected residuals tend to converge after several iterations, despite being forced by different precipitation datasets. The main influence of forcing data is manifested in the omission residuals. As expected, the omission residuals term is simply an approximation of the missing water fluxes or storages in the water budget equation, which can vary depending on the datasets chosen to characterize the equation. In Fig. 12e, the omission residuals driven by Daymet stabilize around 12.5mm, whereas those driven by TRMM stabilize around 6.5mm. Such discrepancy can be further highlighted in the comparison of the residuals time series (Fig. S10). Further investigation would be required to better understand the omission residuals from a physical perspective. For example, a distributed hydrological model with representation of subsurface later flow process will allow us to identify the magnitude of inter-basin interactions; a more detailed description of water budget equation in data-rich environments can help us examine the sources of omission errors. This is undoubtedly important, but not the focus here. In summary, the above results suggest that the correction is minimally sensitive to the choice of forcing, demonstrating the robustness of the correction results.

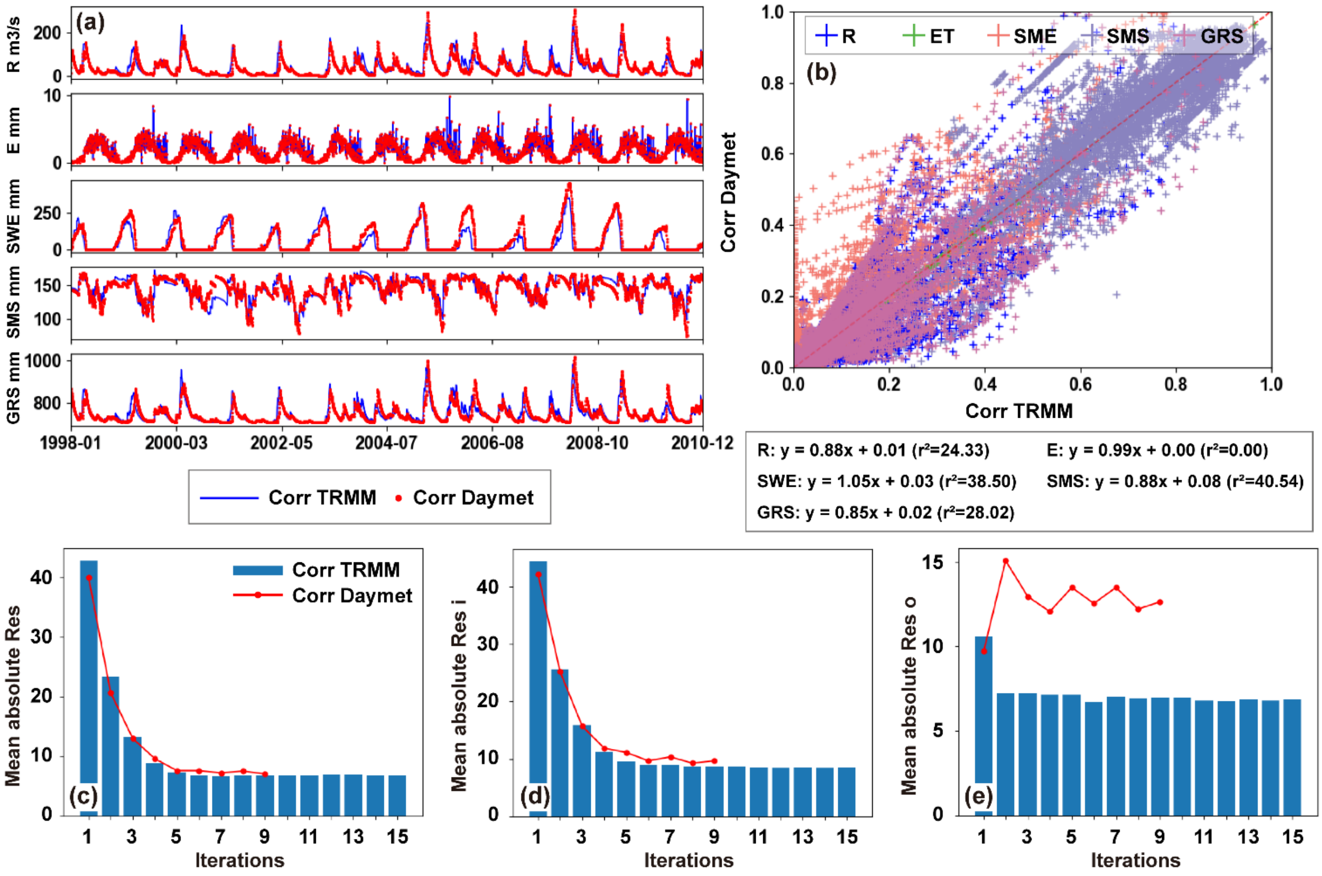

Figure 12. Comparison of correction results based on different forcing datasets (TRMM and Daymet) at basin 1013500. (a-b) Corrected time series of five water budget variables. (c-e) Variation of long-term mean absolute values of three residuals with correction iterations at the monthly scale. The unit of residuals is “mm”.

5.2.2 Uncertainty of model structure

The characterization of physical hydrological processes through modelling constitutes the foundation of the correction framework. The internal model structure is the primary constraint for achieving water budget closure, and thus it is crucial for the final correction results. The selection of the lumped model (i.e., the HBV model) is intended to facilitate the application in large sample basins to derive more general conclusions, as has also been done in many previous large sample hydrology studies

(Gupta et al., 2014). The reliability of model simulations has been confirmed by multi-objective evaluation. However, whether the spatial distribution of model performance is intrinsically related to the model structure is crucial to the robustness of the current work.

To address the question, we first compared the model performance with other studies that employed different models. As illustrated in Fig. C1, the model behaviour exhibits strong spatial organization, with unreliable simulations primarily concentrated in the central and western regions of CONUS. This spatial distribution of prediction skill broadly agrees with many previous studies. Brunner et al. (2021) classified this region as an intermittent regime and attribute the unsatisfactory simulation to the complex day-to-day variation of streamflow. In their work, all four lumped models with different structures (i.e., SAC, HBV, VIC, mHM) supported the inference. In Yan et al. (2023), a more complex land surface model (i.e., CLM5) were utilized for evaluating the uncertainty of runoff prediction, they reported that the Southwest and Central U.S. showed the poorest prediction skill. A notable pioneering research is by Knoben et al. (2020), who evaluated runoff predictability in CAMELS basins using 36 hydrological models with different structures. After conducting a comprehensive analysis, they generated a multi-model runoff prediction performance map, which aligns closely with the results of this study. Therefore, we deduce that the spatial disparities in model performance, or predictability, predominantly depend on basin and climatic conditions rather than model structure. In other words, the HBV model is reliable in the context of this study.

To further substantiate the above inference, we categorized basins into four groups based on model performance in runoff and compared the inter-group differences in six types of basin and climatic characteristics (i.e., climate, hydrology, geology, topography, soil and vegetation). The four groups consist of: unreliable performance, reliable performance, below-average performance, and above-average performance. First, the two sample t-test at the 5% level was conducted to examine whether there are significant differences in each characteristics indicator between the unreliable and reliable groups. The indicators exhibit a statistically significant difference were then presented and compared in Fig. S11 and S12. For clarity, here we list indicators whose inter-group difference greater than 30% in terms of median cumulative probability: mean precipitation, mean potential evapotranspiration, aridity index (climate); proportion of silt (geology-soil); mean streamflow, runoff coefficient, frequency of high-flow days (hydrology); and all vegetation indicators (vegetation). The significant inter-group differences in these indicators highlight critical basin and climatic characteristics pivotal to the successful modelling of the hydrology system, providing convincing evidence for our inference. In summary, basins with the following characteristics typically pose challenges to simulate: arid regions with low precipitation and high potential evaporation, resulting in a low runoff ratio and frequent alternation between zero flow and high flow. Vegetation in these basins tends to consist of lower vegetation types and lack forests.

The distinctive perspective of this work lies in utilizing the physical processes described by hydrological model to constrain multisource datasets, thereby enhancing water budget closure among them. In particular, our next priority is to incorporating more complex models to examine the PHPM-MDCF in different basins with specific hydro-meteorological conditions. For instance, distributed hydrological models and hybrid models (ML-HM) are valuable tools that can improve our understanding of water budget closure through more detailed physical processes representation (Liao and Barros, 2022; Wang and Gupta, 2024).

6 Conclusions

Advanced measurement techniques open new opportunities for modern hydrological research. However, due to the lack of consistent data production protocols and evaluation standards, physical inconsistencies are prevalent in multisource datasets in the form of water budget residuals. Such inconsistencies undermine our confidence in data reliability and compromise the robustness of hydrological inferences rely on these datasets. In this study, we proposed a multisource datasets correction framework, the PHPM-MDCF, to achieve water budget closure through physical hydrological processes modelling. Build upon the decomposition of total water residuals and the iterative multi-objective calibration, the framework has the ability to reduce the inconsistency residuals among multisource datasets and promote convergence between the simulation and measurement systems. We demonstrated the spatiotemporal distribution of water budget residuals and the efficiency of the PHPM-MDCF across 475 COUNS basins selected by hydrological simulation reliability. Several noise experiments were conducted to examined the credibility of the correction. Furthermore, we explored potential factors influencing the distribution of residuals in relation to the basin area and hydro-meteorological conditions The major study findings are summarized as follows:

1. The results from water budget residuals decomposition indicate that inconsistency residuals dominate the total water budget residuals, showing highly consistent spatiotemporal distributions. In spatial terms, both demonstrate an east-west gradient and concentration of low values along the western coastline and eastern inland basins within CONUS. Temporally, they exhibit negative trends in the cold seasons and positive trends in the warm seasons. On the contrary, the omission residuals, which account for the water quantities omitted in the original water budget equation, have different drivers and thus exhibit distinct distributions compared to the former. This component constitutes a relatively small proportion of the total budget residuals.
2. The PHPM-MDCF demonstrates satisfactory correction efficiency, with an average reduction percentage of 49% in total water budget residuals across all 475 basins after correction. In certain basins, this reduction can exceed 80% (i.e., 84% in basin 1013500). The correction efficiency shows a latitudinal-dependent pattern, with greater absolute values in high latitude regions. The results from noise experiments validate the credibility of the correction framework. Both sing-point extreme noise and Gaussian white noise sequence have limited impact on final correction results. The correction applied to extreme noises in one variable will not propagate to other variables, thereby avoiding the generation of unreasonable values.

3. The water budget non-closure phenomena exhibit noticeable scale effects. As the basin area increases, water budget residuals show a decreasing trend. This highlights the need for careful consideration of the water balance assumption when applying multisource datasets for hydrological inference in small basins. Moreover, there is a significant relationship between water budget closure and hydro-meteorological conditions. Wet regions with high precipitation and runoff coefficients typically struggle to achieve water budget closure.

For the first time, this study presents a correction approach to achieve water budget closure based on the physical hydrological modelling. However, the Bayesian philosophy underlying the approach have been implicit in many previous methods, such as atmospheric reanalysis. The only thing we can rely on is our prior knowledge; therefore, continuously promoting convergence between knowledge and measurement systems is crucial for enhancing our confidence. An obvious extension of this research is the inclusion of more disciplines, both within the atmospheric science and broader earth sciences. This contributes to a better understanding in the era of big data of the distinctions and correlations between simulations, measurements, and reality.

Appendix A: Implementation details of the HBV model

Figure A1 illustrates the basic structure of the HBV model, encompassing three modules (i.e., snow routine, soil moisture routine and runoff routine) and three runoff components: quick runoff, interflow and baseflow. The cumulative sum of these runoff components constitutes total runoff, which is routed through a triangular unit hydrograph (UH). At each model run step, the streamflow at the outlet of the basin is determined. The HBV model is driven by daily precipitation (from TRMM), average temperature (from CAMELS) and potential evaporation (from GLEAM), enabling the simulation of various hydrological fluxes and state variables, including streamflow, soil moisture storage, groundwater reservoir storage, evaporation and SWE. Table A1 lists the free parameters slated for calibration in the HBV model, providing their descriptions and respective ranges.

The period from 1998 to 2000 is looped five times for model spin-up and the subsequent 10-year period is used for model calibration. After each calibration, the optimal parameters set is selected from the Pareto fronts. Finally, these optimal parameters are applied to the entire 12-year period to yield the best simulation, thus facilitating the multisource datasets correction.

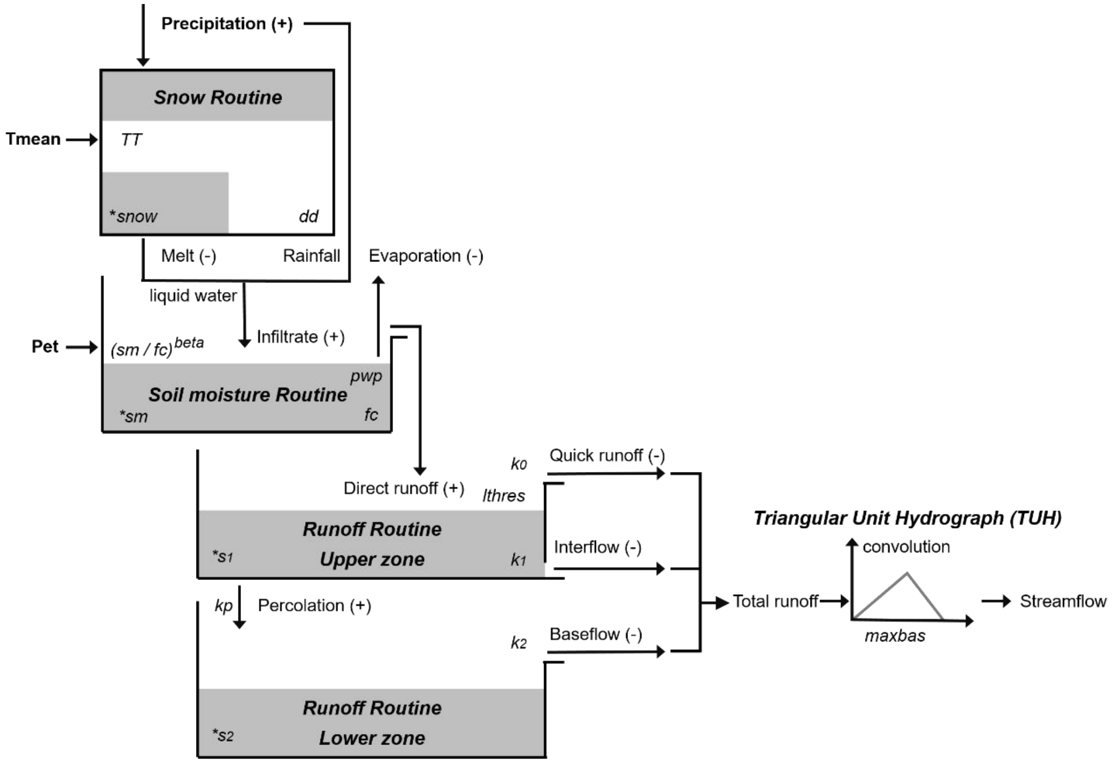

660

Figure A1. Schematic structure of the HBV model. The variables marked with asterisk (*) denote water storage, whereas those annotated with positive (+) and negative (-) signs represent the inputs and outputs of the storage.

Table A1. The description and ranges of free parameters in the HBV model for calibration.

Parameter	Unit	Description	Min	Max
DD	[mm °C^{-1} d^{-1}]	Degree-day factor	1.0	10.0
TT	[°C]	Threshold temperature for snowmelt initiation	-2.5	2.5
Beta	[-]	Shape coefficient	1.0	8.0
FC	[mm]	Filed capacity	10.0	600.0
K_0	[d^{-1}]	Recession coefficient of the quick runoff	0.1	0.8
K_1	[d^{-1}]	Recession coefficient of the interflow	0.01	0.5
K_2	[d^{-1}]	Recession coefficient of the baseflow	0.001	0.15
K_p	[d^{-1}]	Recession coefficient of the percolation	0.001	5.0
PWP	[-]	Soil permanent wilting point as a fraction of FC	0.2	1.0
HL	[mm]	Threshold water level for near-surface flow	10.0	200.0
maxbas	[d]	Weighting parameter of triangular unit hydrograph	1	10

Appendix B: Evaluation metrics used for model calibration

The Kling-Gupta Efficiency (KGE) metric provides a comprehensive measure of the similarity between simulations and measurements by incorporating three components: correlation, the ratio of standard deviations, and the ratio of means. It has been demonstrated to exhibit superior performance in calibrating hydrological models (Knoben et al., 2020; Aerts et al., 2022). The Pearson correlation coefficient (r) quantifies the extent of shared information between simulations and measurements, characterized by its insensitivity to amplitude and mean values (Lorenz et al., 2014). Thus, it is suitable for evaluating variables that may exhibit mean differences between simulations and measurements, such as SMS and GRS. The Root Mean Square Error (RMSE) is a widely used evaluation metric in hydrological modelling. Despite it is not a normalized metric, its calculation does not involve division, making it particularly suitable for evaluating variables like SWE, which may be a sequence entirely consisting of zeros. Based on the simulated and measured values of the target variables, the three metrics can be calculated using the following formulas:

$$KGE = 1 - \sqrt{(r-1)^2 + (\frac{\sigma_{sim}}{\sigma_{obs}} - 1)^2 + (\frac{\mu_{sim}}{\mu_{obs}} - 1)^2}, \tag{B1}$$

$$r = \frac{\sum_{i=1}^{n}(V_{obs}^{i} - \overline{V_{obs}})(V_{sim}^{i} - \overline{V_{sim}})}{\sqrt{\sum_{i=1}^{n}(V_{obs}^{i} - \overline{V_{obs}})^2}\sqrt{\sum_{i=1}^{n}(V_{sim}^{i} - \overline{V_{sim}})^2}}, \tag{B2}$$

$$RMSE = \sqrt{\frac{1}{n}\sum_{i=1}^{n}(V_{sim}^{i} - V_{obs}^{i})^2}, \tag{B3}$$

where σ is the standard deviation and μ is the mean; V^i is the target variable at time step i and n is the length of the sequence. The subscripts "sim" and "obs" denotes the simulation and measurements of the variable, respectively. The range and optimal values of the evaluation metrics are detained in Table B1.

Table B1. Description of evaluation metrics, including ranges and optimal values.

Metrics	Full name	Variables to be evaluated	Range	Optimal value
KGE	Kling-Gupta Efficiency	Runoff, evaporation	$(-\infty, 1]$	1.0
r	Pearson correlation coefficient	Soil moisture storage, groundwater reservoir storage	$[-1,1]$	1.0
RMSE	Root Mean Square Error	Snow water equivalent	$[0, +\infty)$	0.0

Appendix C: Simulation performance of the HBV model across CAMELS basins

In this Appendix we present the simulation performance of the HBV model on 653 CAMELS basins. As shown in Fig. C1, the performance of five target variables including runoff, evaporation, soil moisture storage, groundwater reservoir storage, and snow water equivalent, is described by three metrics (i.e., KGE, r, and RMSE). The gradient from white to deep blue indicates progressively better simulation performance. In contrast, red highlights basins of unreliable simulation, determined by a KGE of less than -0.41 and r value failing the significance test at the 5% level. Table C1 summarizes the multivariable simulation performance of the HBV model across all basins.

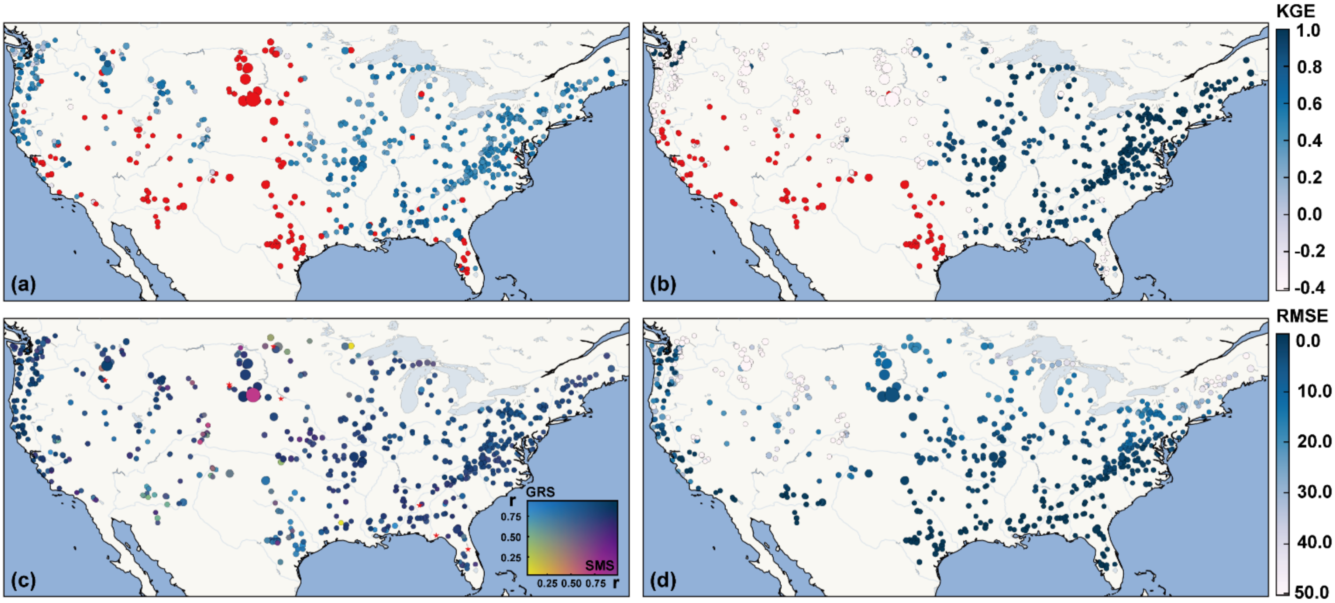

690 **Figure C1.** The multi-objective simulation performances of the HBV model across the CAMELS basins. Results are based on (a) runoff, (b) evaporation, (c) soil moisture storage and groundwater reservoir storage, and (d) snow water equivalent. Red dots represent unreliable simulation performance, and the size of points is proportional to the basin area. The unit of RMSE is "mm".

Table C1. Performances of the HBV model in terms of five target variables across the CAMELS basins. The last row presents the number and proportion of basins where all target variables are reliably simulated. The unit of RMSE in the table is "mm".

Variables	Median performance (KGE, r, RMSE)	Range (KGE, r, RMSE)	Reliable Simulations Count (Basins)	Reliable Proportion (%)
Streamflow	0.50	-0.40~0.88	499	76.42%
ET	0.94	-0.40~0.99	548	83.92%
SMS	0.80	0.07~0.95	645	98.77%
GRS	0.72	0.02~0.95	653	100.00%
SWE	5.97	0.00~353.34	-	-
All variables	-	-	475	72.74%

695

Data availability

All data used in this study is freely available through public open-source platforms. The TRMM 3B42V7 precipitation production is available at the NASA Goddard Earth Sciences Data and Information Services Center (GES DISC) website (https://disc.gsfc.nasa.gov/datasets/TRMM_3B42_Daily_7/summary, Huffman et al., 2016); the GLEAM evaporation and potential evaporation data from Martens et al. (2017), are available at https://www.gleam.eu/; the EAR5 Land data are available at https://cds.climate.copernicus.eu (Mu ñoz Sabater et al., 2021); the GlobSnow v3.0 SWE data can be downloaded from the official website: https://www.globsnow.info/swe/ (Luojus et al., 2021).

The basin characteristics and daily streamflow records come from the Catchment Attributes and Meteorology for Large-sample Studies (CAMELS) dataset, which can be obtained from https://ncar.github.io/hydrology/datasets/CAMELS_attributes (Addor et al., 2017).

Author contributions

XDZ: conceptualization, data curation, formal analysis, writing – original draft. DEL: conceptualization, supervision, writing – review and editing. SZH, HW, XM: supervision and review.

Competing interests

The authors declare that they have no conflict of interest.

Acknowledgements

This work was performed as part of the PhD project of XudongZheng.

Financial support

This study was financially supported by the National Key Research and Development Program of China (2022YFF1302200) and the National Natural Science Foundation of China (Grant Nos. 52279025 and 42071335).

References

Abhishek, Kinouchi, T., Abolafia-Rosenzweig, R., and Ito, M.: Water Budget Closure in the Upper Chao Phraya River Basin, Thailand Using Multisource Data, Remote Sensing, 14, 10.3390/rs14010173, 2022.

Abolafia-Rosenzweig, R., Pan, M., Zeng, J., and Livneh, B.: Remotely sensed ensembles of the terrestrial water budget over major global river basins: An assessment of three closure techniques, Remote Sensing of Environment, 252, 10.1016/j.rse.2020.112191, 2020.

Addor, N., Newman, A. J., Mizukami, N., and Clark, M. P.: The CAMELS data set: catchment attributes and meteorology for large-sample studies, Hydrology and Earth System Sciences, 21, 5293-5313, 10.5194/hess-21-5293-2017, 2017.

Aerts, J., Hut, R., van de Giesen, N., Drost, N., Verseveld, W., Weerts, A., and Hazenberg, P.: Large-sample assessment of varying spatial resolution on the streamflow estimates of the wflow_sbm hydrological model, Hydrology and Earth System Sciences, 26, 4407-4430, 10.5194/hess-26-4407-2022, 2022.

Ansari, R., Liaqat, M. U., and Grossi, G.: Evaluation of gridded datasets for terrestrial water budget assessment in the Upper Jhelum River Basin-South Asia, Journal of Hydrology, 613, 128294, 10.1016/j.jhydrol.2022.128294, 2022.

Balsamo, G., Viterbo, P., Beljaars, A., Hurk, B., Hirschi, M., Betts, A., and Scipal, K.: A Revised Hydrology for the ECMWF Model: Verification from Field Site to Terrestrial Water Storage and Impact in the Integrated Forecast System, Journal of Hydrometeorology, 10, 623, 10.1175/2008JHM1068.1, 2009.

Bergström, S.: Development and Application of a Conceptual Runoff Model for Scandinavian Catchments, 1976.

Beven, K.: Benchmarking Hydrological Models for an Uncertain Future, Hydrol Process, 10.1002/hyp.14882, 2023.

Brunner, M. I., Melsen, L. A., Wood, A. W., Rakovec, O., Mizukami, N., Knoben, W. J. M., and Clark, M. P.: Flood spatial coherence, triggers, and performance in hydrological simulations: large-sample evaluation of four streamflow-calibrated models, Hydrology and Earth System Sciences, 25, 105-119, 10.5194/hess-25-105-2021, 2021.

Clark, M., Lamontagne, J., Mizukami, N., Knoben, W., Tang, G., Gharari, S., Freer, J., Whitfield, P., Shook, K., and Papalexiou, S. M.: The Abuse of Popular Performance Metrics in Hydrologic Modeling, Water Resources Research, 57, 10.1029/2020WR029001, 2021.

Deb, K., Pratap, A., Agarwal, S., and Meyarivan, T.: A fast and elitist multiobjective genetic algorithm: NSGA-II, IEEE Trans. on Evol, IEEE Transactions on Evolutionary Computation - TEC, 6, 2002.

Feng, D., Liu, J., Lawson, K., and Shen, C.: Differentiable, Learnable, Regionalized Process-Based Models With Multiphysical Outputs can Approach State-Of-The-Art Hydrologic Prediction Accuracy, Water Resources Research, 58, 10.1029/2022WR032404, 2022.

Fortin, F.-A., De Rainville, F.-M., Gardner, M. A., Parizeau, M., and Gagné, C.: DEAP: Evolutionary algorithms made easy, Journal of Machine Learning Research, Machine Learning Open Source Software, 13, 2171-2175, 2012.

Gordon, B., Crow, W., Konings, A., Dralle, D., and Harpold, A.: Can We Use the Water Budget to Infer Upland Catchment Behavior? The Role of Data Set Error Estimation and Interbasin Groundwater Flow, Water Resources Research, 58, 10.1029/2021WR030966, 2022.

Gupta, H., Perrin, C., Blöschl, G., Montanari, A., Kumar, R., Clark, M., and Andréassian, V.: Large-sample hydrology: a need to balance depth with breadth, Hydrology and Earth System Sciences, 18, 10.5194/hess-18-463-2014, 2014.

Gupta, H. V., Kling, H., Yilmaz, K. K., and Martinez, G. F.: Decomposition of the mean squared error and NSE performance criteria: Implications for improving hydrological modelling, Journal of Hydrology, 377, 80-91, 2009.

Hoeltgebaum, L. and Dias, N.: Evaluation of the storage and evapotranspiration terms of the water budget for an agricultural watershed using local and remote-sensing measurements, Agricultural and Forest Meteorology, 341, 10.1016/j.agrformet.2023.109615, 2023.

Huang, P., Wang, G., Guo, L., de Mello, C., Li, K., Ma, J., and Sun, S.: Most Global Gauging Stations Present Biased Estimations of Total Catchment Discharge, Geophysical Research Letters, 50, 10.1029/2023GL104253, 2023.

Huffman, G. J., D.T. Bolvin, E.J. Nelkin, a., and Adler, R. F.: TRMM (TMPA) Precipitation L3 1 day 0.25 degree x 0.25 degree V7 [dataset], 10.5067/TRMM/TMPA/DAY/7, 2016.

Kabir, T., Pokhrel, Y., and Felfelani, F.: On the Precipitation-Induced Uncertainties in Process-Based Hydrological Modeling in the Mekong River Basin, Water Resources Research, 58, 10.1029/2021WR030828, 2022.

Kauffeldt, A., Halldin, S., Rodhe, A., Xu, C. Y., and Westerberg, I. K.: Disinformative data in large-scale hydrological modelling, Hydrology and Earth System Sciences, 17, 2845-2857, 2013.

Kittel, C. M. M., Nielsen, K., Tottrup, C., and Bauer-Gottwein, P.: Informing a hydrological model of the Ogooue with multi-mission remote sensing data, Hydrology and Earth System Sciences, 22, 1453-1472, 2018.

Knoben, W., Freer, J., Peel, M., Fowler, K., and Woods, R.: A Brief Analysis of Conceptual Model Structure Uncertainty Using 36 Models and 559 Catchments, Water Resources Research, 56, e2019WR025975, 10.1029/2019WR025975, 2020.

Lehmann, F., Vishwakarma, B., and Bamber, J.: How well are we able to close the water budget at the global scale?, Hydrology and Earth System Sciences, 26, 35-54, 10.5194/hess-26-35-2022, 2022.

Liao, M. and Barros, A.: Toward optimal rainfall – Hydrologic QPE correction in headwater basins, Remote Sensing of Environment, 279, 113107, 10.1016/j.rse.2022.113107, 2022.

Lorenz, C., Kunstmann, H., Devaraju, B., Tourian, M., Sneeuw, N., and Riegger, J.: Large-Scale Runoff from Landmasses: A Global Assessment of the Closure of the Hydrological and Atmospheric Water Balances, Journal of Hydrometeorology, 15, 10.1175/JHM-D-13-0157.1, 2014.

Luo, Z., Li, H., Zhang, S., Wang, L., Wang, S., and Wang, L.: A Novel Two-Step Method for Enforcing Water Budget Closure and an Intercomparison of Budget Closure Correction Methods Based on Satellite Hydrological Products, Water Resources Research, 59, 10.1029/2022WR032176, 2023.

Luo, Z., Shao, Q., Wan, W., Li, H., Xi, C., Zhu, S., and Ding, X.: A new method for assessing satellite-based hydrological data products using water budget closure, Journal of Hydrology, 594, 125927, 10.1016/j.jhydrol.2020.125927, 2020.

Luojus, K., Pulliainen, J., Takala, M., Lemmetyinen, J., Mortimer, C., Derksen, C., Mudryk, L., Moisander, M., Hiltunen, M., Smolander, T., Ikonen, J., Cohen, J., Salminen, M., Norberg, J., Veijola, K., and Venäläinen, P.: GlobSnow v3.0 Northern Hemisphere snow water equivalent dataset, Scientific Data, 8, 10.1038/s41597-021-00939-2, 2021.

Lv, M., Ma, Z., Yuan, X., Lv, M., Li, M., and Zheng, Z.: Water budget closure based on GRACE measurements and reconstructed evapotranspiration using GLDAS and water use data for two large densely-populated mid-latitude basins, Journal of Hydrology, 547, 10.1016/j.jhydrol.2017.02.027, 2017.

Martens, B., Miralles, D., Hans, L., van der Schalie, R., de Jeu, R., Fernández-Prieto, D., Beck, H., Dorigo, W., and Verhoest, N.: GLEAM v3: Satellite-based land evaporation and root-zone soil moisture, Geosci Model Dev, 10, 10.5194/gmd-10-1903-2017, 2017.

Miralles, D., Holmes, T., de Jeu, R., Gash, J., Meesters, A., and Dolman, H.: Global land-surface evaporation estimated from satellite-based observations, Hydrology and Earth System Sciences, 15, 453-469, 10.5194/hess-15-453-2011, 2011.

Mostafaie, A., Forootan, E., Safari, A., and Schumacher, M.: Comparing multi-objective optimization techniques to calibrate a conceptual hydrological model using in situ runoff and daily GRACE data, Computat Geosci, 22, 789-814, 2018.

Munier, S., Aires, F., Schlaffer, S., Prigent, C., Papa, F., Maisongrande, P., and Pan, M.: Combining datasets of satellite retrieved products for basin-scale water balance study. Part II: Evaluation on the Mississippi Basin and closure correction model, Journal of Geophysical Research, 10.1002/2014JD021953, 2014.

Muñoz Sabater, J., Dutra, E., Agusti-Panareda, A., Albergel, C., Arduini, G., Balsamo, G., Boussetta, S., Choulga, M., Harrigan, S., Hersbach, H., Martens, B., Miralles, D., Piles, M., Rodriguez-Fernandez, N., Zsótér, E., Buontempo, C., and Thépaut, J. N.: ERA5-Land: A state-of-the-art global reanalysis dataset for land applications, Earth System Science Data, 13, 4349-4383, 10.5194/essd-13-4349-2021, 2021.

Nearing, G., Kratzert, F., Sampson, A., Pelissier, C., Klotz, D., Frame, J., Prieto, C., and Gupta, H.: What Role Does Hydrological Science Play in the Age of Machine Learning?, Water Resources Research, 57, 10.1029/2020WR028091, 2021.

Newman, A. J., Clark, M. P., Sampson, K., Wood, A., Hay, L. E., Bock, A., Viger, R. J., Blodgett, D., Brekke, L., Arnold, J. R., Hopson, T., and Duan, Q.: Development of a large-sample watershed-scale hydrometeorological data set for the contiguous USA: data set characteristics and assessment of regional variability in hydrologic model performance, Hydrology and Earth System Sciences, 19, 209-223, 10.5194/hess-19-209-2015, 2015.

Pan, M. and Wood, E.: Data Assimilation for Estimating the Terrestrial Water Budget Using a Constrained Ensemble Kalman Filter, Journal of Hydrometeorology - J HYDROMETEOROL, 7, 10.1175/JHM495.1, 2006.

Penning de Vries, M., Fennig, K., Schröder, M., Trent, T., Bakan, S., Roberts, J., and Robertson, F.: Intercomparison of freshwater fluxes over ocean and investigations into water budget closure, Hydrology and Earth System Sciences, 25, 121-146, 10.5194/hess-25-121-2021, 2021.

Petch, S., Dong, B., Quaife, T., King, R., and Haines, K.: Water and energy budgets over hydrological basins on short and long timescales, Hydrology and Earth System Sciences, 27, 1723-1744, 10.5194/hess-27-1723-2023, 2023.

Peters-Lidard, C., Clark, M., Samaniego, L., Verhoest, N., van Emmerik, T., Uijlenhoet, R., Achieng, K., Franz, T., and Woods, R.: Scaling, Similarity, and the Fourth Paradigm for Hydrology, Hydrology and Earth System Sciences, 21, 3701-3713, 10.5194/hess-21-3701-2017, 2017.

Refsgaard, J. C., Stisen, S., and Koch, J.: Hydrological process knowledge in catchment modelling - Lessons and perspectives from 60 years development, Hydrol Process, 36, 2022.

Robinson, E. and Clark, D.: Using Gravity Recovery and Climate Experiment data to derive corrections to precipitation data sets and improve modelled snow mass at high latitudes, Hydrology and Earth System Sciences, 24, 1763-1779, 10.5194/hess-24-1763-2020, 2020.

Sahoo, A., Pan, M., Troy, T., Vinukollu, R., Sheffield, J., and Wood, E.: Reconciling the global terrestrial water budget using satellite remote sensing, Remote Sensing of Environment, 115, 1850-1865, 10.1016/j.rse.2011.03.009, 2011.

Sivapalan, M. and Blöschl, G.: The Growth of Hydrological Understanding: Technologies, Ideas and Societal Needs Shape the Field, Water Resources Research, 53, 10.1002/2017WR021396, 2017.

Stoffelen, A.: Error Modeling and Calibration; Towards the true surface wind speed, J. Geophys. Res., 103, 7,755-757,766, 10.1029/97JC03180, 1998.

Tang, G., Clark, M., Papalexiou, S. M., Ma, Z., and Hong, Y.: Have satellite precipitation products improved over last two decades? A comprehensive comparison of GPM IMERG with nine satellite and reanalysis datasets, Remote Sensing of Environment, 240, 111697, 10.1016/j.rse.2020.111697, 2020.

Wang, J., Zhuo, L., Han, D., Liu, Y., and Rico-Ramirez, M.: Hydrological Model Adaptability to Rainfall Inputs of Varied Quality, Water Resources Research, 59, 10.1029/2022WR032484, 2023.

Wang, Y. H. and Gupta, H.: A Mass-Conserving-Perceptron for Machine-Learning-Based Modeling of Geoscientific Systems, Water Resources Research, 60, 10.1029/2023WR036461, 2024.

Weligamage, H., Fowler, K., Peterson, T., Saft, M., Peel, M., and Ryu, D.: Partitioning of Precipitation Into Terrestrial Water Balance Components Under a Drying Climate, Water Resources Research, 59, 10.1029/2022WR033538, 2023.

Yan, H., Sun, N., Eldardiry, H., Thurber, T., Reed, P., Malek, K., Gupta, R., Kennedy, D., Swenson, S., Hou, Z., Cheng, Y., and Rice, J.: Large Ensemble Diagnostic Evaluation of Hydrologic Parameter Uncertainty in the Community Land Model Version 5 (CLM5), Journal of Advances in Modeling Earth Systems, 15, 10.1029/2022MS003312, 2023.

Zhang, Y., Pan, M., and Wood, E.: On Creating Global Gridded Terrestrial Water Budget Estimates from Satellite Remote Sensing, in: Remote Sensing and Water Resources, Space Sciences Series of ISSI, 59-78, 10.1007/978-3-319-32449-4_4, 2016.